A radio continuum study of the Magellanic Clouds, VI. Discrete sources common to radio and X-ray surveys of the Magellanic Clouds

Filipovic, M.D.; Pietsch, W.; Haynes, R.F.; White, G.L.; Jones, P.A.; Wielebinski, R.; Klein, U.; Dennerl, K.; Kahabka, P.; Lazendic, J.S.

Published in:
Astronomy and Astrophysics Supplement Series

ASTRONOMY & ASTROPHYSICS
SUPPLEMENT SERIES

JANUARY II **1998**, PAGE 119

Astron. Astrophys. Suppl. Ser. **127,** 119-138 (1998)

A radio continuum study of the Magellanic Clouds

VI. Discrete sources common to radio and X-ray surveys of the Magellanic Clouds*

M.D. Filipović[1,2,3], W. Pietsch[3], R.F. Haynes[2,1], G.L. White[1], P.A. Jones[1], R. Wielebinski[4], U. Klein[5], K. Dennerl[3], P. Kahabka[3,6], and J.S. Lazendić[7,1]

[1] University of Western Sydney, Nepean, P.O. Box 10, Kingswood, NSW 2747, Australia
fica@st.nepean.uws.edu.au; p.jones@st.nepean.uws.edu.au; g.white@st.nepean.uws.edu.au
[2] Australia Telescope National Facility, CSIRO, P.O. Box 76, Epping, NSW 2121, Australia
mfilipovic@atnf.csiro.au; rhaynes@atnf.csiro.au
[3] Max-Planck-Institut für extraterrestrische Physik, Giessenbachstraße, D-85740 Garching, Germany
wnp@mpe-garching.mpg.de; kod@mpe-garching.mpg.de
[4] Max-Planck-Institut für Radioastronomie, Auf dem Hügel 69, D-53121 Bonn, Germany
p647gbr@mpifr-bonn.mpg.de
[5] Radioastronomisches Institut der Universitat Bonn, Auf dem Hügel 71, D-53121 Bonn, Germany
p213ukl@astro.uni-bonn.de
[6] Center for High Energy Astrophysics, University of Amsterdam, Kruislaan 403, NL-1098 SJ Amsterdam, The Netherlands
ptk@astro.uva.nl
[7] Department of Astronomy, University of Belgrade, Studentski trg 13, 11000 Beograd, Serbia, Yugoslavia
jasmina@st.nepean.uws.edu.au

Received March 3; accepted April 24, 1997

Abstract. By comparing Parkes telescope radio surveys with the X-ray ROSAT All-Sky Survey (RASS) we have found 71 discrete sources of both radio and X-ray emission in the Large Magellanic Cloud (LMC). These 71 sources are mainly supernova remnants (SNRs) and SNR candidates (36), and background sources (27). For six of the sources we have no proposed identification and the other two are H II regions. A source-intensity comparison of the radio and X-ray sources shows very little correlation, but we note that the strongest SNRs at both radio and X-ray frequencies are young SNRs from Population I. Six new LMC SNR candidates are proposed. From the radio flux density of the SNRs we have estimated the SNR birth rate to be one every 100 ($\pm$20) yr and the star-formation rate (SFR) to be 0.7 ($\pm$0.2) $M_{\odot}\,\mathrm{yr}^{-1}$.

A similar comparison was undertaken for the Small Magellanic Cloud (SMC), but instead of the RASS we used a roster of pointed observations made with the ROSAT Position Sensitive Proportional Counter (PSPC). This comparison resulted in 27 sources in common between the Parkes radio and ROSAT PSPC surveys. Two new SMC sources are proposed for SNR candidates. The SMC SNR birth rate was estimated to be one every 350 ($\pm$70) yr and the SFR was estimated to be 0.15 ($\pm$0.05) $M_{\odot}\,\mathrm{yr}^{-1}$.

Key words: galaxies: Magellanic Clouds — radio continuum: galaxies — X-rays: galaxies — ISM: supernova remnants (SNRs) — ISM: H II regions

1. Introduction

The Magellanic Clouds (MCs) are excellent laboratories for studying discrete sources owing to their proximity to our own Galaxy. Most discrete radio sources in spiral and irregular galaxies are SNRs and H II regions. SNRs are usually observed as strong X-ray sources, whereas H II regions are generally weak X-ray emitters. It is well known that SNRs and X-ray binaries often occur in large H II regions and hence H II regions sometimes appear in X-ray surveys.

The first high-frequency radio detection of discrete sources in the MCs was made by McGee & Milton (1966) at 1.4 GHz, which opened a new era in extra galactic research. Pioneering X-ray surveys of the LMC have been

Send offprint requests to: M.D. Filipović

* Tables 2 and 3 are also available electronically at the CDS via anonymous ftp to cdsarc.u-strasbg.fr (130.79.128.5) or via http: //cdsweb.u-strasbg.fr/Abstract.html

presented in Long et al. (1981) (LHG catalogue) and in Wang et al. (1991) (W catalogue). The SMC X-ray surveys can be found in Seward & Mitchell (1981) (1E catalogue), Inoue et al. (1983) (IKT catalogue), Bruhweiler et al. (1987) and in Wang & Wu (1992). All these surveys are based on observations made with the Einstein satellite.

Almost half of the X-ray sources in the LMC field catalogued by Wang et al. (1991) were confirmed as SNRs, H II regions or X-ray binaries. The other half are foreground stars or background objects (e.g. clusters of galaxies, radio galaxies, quasars). In the Wang & Wu (1992) survey, 24 out of 70 sources towards the SMC are intrinsic to the SMC.

These earlier studies provided a good basis for a new generation of radio and X-ray surveys of the MCs. Recent Parkes radio surveys of the MCs are now available: Haynes et al. (1991), Filipović et al. (1995; hereafter Paper IV), Filipović et al. (1996, hereafter Paper IVa), Filipović et al. (1997a, hereafter Paper V) and Filipović (1996). At X-ray frequencies, Pietsch et al. (in preparation) have prepared a list of sources towards the LMC from the X-ray ROSAT All-Sky Survey (RASS; Pietsch & Kahabka 1993) and Kahabka et al. (in preparation) presented a list of sources towards the SMC from the ROSAT Position Sensitive Proportional Counter (PSPC).

There are several other high-resolution surveys of the MCs in progress. At radio frequencies, a neutral-hydrogen survey at 1.4 GHz and continuum surveys at 1.4 and 2.3 GHz have been made with the Compact Array of the Australia Telescope National Facility (Staveley-Smith et al. 1997). At X-ray frequencies there are the ROSAT PSPC and HRI pointed observations (Snowden & Petre 1994) and the ASCA X-ray observations of some MCs SNRs (Hughes et al. 1995).

In this paper we compare sources common to the available radio and X-ray surveys using primarily the radio data of Papers IV, IVa and V and X-ray data of Pietsch et al. (in preparation) and Kahabka et al. (in preparation). We classify each source as either SNR, H II region, X-ray binary, background object or foreground star. In Sect. 2 we briefly discuss discrete radio and X-ray sources. In Sects. 3 and 4 we analyse and discuss all discrete sources common to the radio surveys and the ROSAT X-ray surveys. Finally, in Sect. 5 we discuss the radio–to–X-ray source-intensity relationships for all sources in common towards the MCs, with special emphasis on the LMC SNRs.

2. Discrete sources towards the MCs

2.1. Discrete radio sources towards the LMC

Catalogues of discrete radio sources towards the LMC at six radio frequencies are presented in Papers IV and IVa of this series and in Filipović (1996). The total number of catalogued radio sources is 483: 192 at 1.40 GHz, 119 at 2.30 GHz, 338 at 2.45 GHz, 373 at 4.75 GHz, 332 at 4.85 GHz and 212 at 8.55 GHz. As clear radio detections, we listed only radio sources that are stronger than 5σ or seen at two or more frequencies.

2.2. Discrete X-ray sources towards the LMC

A catalogue of RASS X-ray sources towards the LMC is published in Pietsch et al. (in preparation). In addition to this catalogue we compared Parkes radio and RASS images and found eight additional X-ray sources which are not catalogued in Pietsch et al. (in preparation). These eight sources are listed in Table 1 which follows the format of the table in Pietsch et al. (in preparation). Source positions, RA and Dec, are given in J2000 coordinates in Col. 2 and Col. 3, respectively. Positional error is given in Col. 4 and the exposure time in Col. 5. The definitions of likelihood existence (LH) (Col. 6), count rate (Col. 7), hardness ratios (HR1) and (HR2) (Cols. 8 and 9, respectively) are the same as in Pietsch et al. (in preparation). Count rates of the sources have been derived for the five standard energy bands: "broad" ($0.11-2.4$ keV), "soft" ($0.11-0.41$ keV), "hard" ($0.52-2.01$ keV), "hard1" ($0.52-0.90$ keV) and "hard2" ($0.91-2.01$ keV). HR1 is defined as HR1 = (hard − soft)/(hard + soft) and HR2 is defined as HR2 = (hard2 − hard1)/(hard2 + hard1). LH is the maximum likelihood of source existence and may be converted into probabilities via $P\sim 1-\mathrm{e}^{(-LH)}$. That means that $LH=9.7$ corresponds to about four Gaussian sigma significance. All sources have $LH\geq 8$.

We believe that a number of other radio sources could have X-ray counterparts, but because most of these sources belong to confused regions, we could not resolve them in the RASS. We expect that these "confused" sources will be resolved in the ROSAT-pointed observations (PSPC) which have better resolution.

We use the common area of the radio and X-ray surveys defined in Paper IV of ∼100 square degrees between RA (B1950) = $04^{\mathrm{h}}23^{\mathrm{m}}$ to $06^{\mathrm{h}}14^{\mathrm{m}}$ and Dec (B1950) = -74° to -64°. In this area we expect about eight sources to have positional coincidence by chance alignment, based on the number of sources at each frequency and $2.5'$ search criterion for coincidence. Also, we have checked this number of chance coincidences by simulation. We shifted one set of positions in either coordinate by 5 to $30'$ and found the number of spurious coincidences to be 9 ± 3 over repeated trials.

We now have 325 RASS sources towards the LMC field defined by the radio surveys (see Sect. 2.1) and we compare these with 483 radio sources in the same field.

2.3. Discrete radio sources towards the SMC

The new catalogues of radio sources in the SMC at five radio frequencies: 1.42 GHz (86 sources), 2.45 GHz (107 sources), 4.75 GHz (99 sources), 4.85 GHz (187 sources) and 8.55 GHz (41 sources) are given in Paper V and in

Table 1. Additional LMC RASS sources found after comparison with Parkes radio data (Paper IV) and not listed in Pietsch et al. (in preparation). Entries in this table follow the format of Pietsch et al. (in preparation)

(1) No.	(2) RA (2000) h m s	(3) Dec (2000) ° ′ ″	(4) P_e (″)	(5) Exposure (s)	(6) LH	(7) Count Rate (cts ks^{-1})	(8) HR1	(9) HR2	(10) Other Names
9001	04 28 36.7	−67 49 10	19	1420	13	4.8 ± 2.5	1.00±0.00	1.00±0.00	PKS B0428 − 679
9002	04 46 09.0	−72 04 53	40	1019	10	12.1 ± 4.9	0.81±0.35	0.68±0.29	
9003	04 54 21.3	−68 00 11	30	2028	8	7.2 ± 2.8	0.35±0.35	0.38±0.36	
9004	05 13 42.2	−67 24 19	29	2293	8	3.2 ± 2.1	1.00±0.00	1.00±0.00	N 30; DEM L112
9005	05 24 10.0	−66 20 54	21	2110	11	4.5 ± 2.4	1.00±0.00	1.00±0.00	N 46; DEM L162
9006	05 28 49.3	−65 39 41	26	3250	8	2.2 ± 1.4	1.00±0.00	0.32±0.43	
9007	05 34 59.3	−64 38 27	47	1827	9	6.9 ± 3.4	0.61±0.38	0.89±0.35	
9008	05 38 34.7	−69 06 06	37	2199	19	27.4 ± 6.8	1.00±0.00	0.32±0.20	30 Dor; N 157A

Filipović (1996). There is a total of 224 radio sources towards the SMC. As clear radio detections, again we listed only radio sources that are stronger than 5σ or seen in at least two frequencies.

2.4. Discrete X-ray sources towards the SMC

A catalogue of the ROSAT PSPC sources in the field of the SMC is published in Kahabka et al. (in preparation) and combines the results of nine pointed observations. These observations (exposure corrected) of the SMC were carried out with the ROSAT PSPC detector in the energy range 0.1 − 0.4 keV and 0.4 − 2.4 keV.

Using the common area of the radio and X-ray surveys ($\sim$ 12 square degrees between RA (B1950) = $00^{\rm h}30^{\rm m}$ to $01^{\rm h}20^{\rm m}$ and Dec (B1950) = $-71°18'$ to $-74°32'$) and the search criterion, we expect about nine sources to have positional coincidence by chance alignment. In this area, there are 86 radio sources from our Parkes radio surveys and they are compared with 248 X-ray PSPC sources from Kahabka et al. (in preparation).

3. Source identification

The comparison of the Parkes radio and the ROSAT X-ray surveys of the LMC resulted in the discovery of 71 sources common to both surveys. A similar comparison was undertaken for the SMC field and resulted in the discovery of 27 sources common to both surveys. Each source lies within $2.5'$ of its counterpart; this is the basic criterion for positive source identification. This criterion was chosen according to the upper limit of positional uncertainties at our 1.4 GHz survey which is $\sim 2'$ at the 1σ level (Paper IV). The most accurate radio positions available are from the highest radio-frequency survey in which the sources appear. These positions were compared with X-ray positions from Pietsch et al. (in preparation) and Kahabka et al. (in preparation).

In Table 2, we present data for the 71 sources in common towards the LMC and in Table 3 we list the 27 sources in common towards the SMC. Columns 2 and 3 of Tables 2 and 3 give the radio-source and X-ray source names respectively. Column 4 lists the source radio flux density at 4.75 GHz (4.85 GHz for the SMC). For eight LMC and five SMC sources the flux density at 4.75 GHz (4.85 GHz for the SMC) was estimated by interpolation from other radio frequencies; these sources are flagged in Col. 4. The X-ray information, count rate and HR2, are listed for each source in Col. 5 and Col. 7 respectively.

Column 6 lists the source radio spectral index (α) and error ($\Delta\alpha$) as defined by the relationship $S_\nu \sim \nu^\alpha$, where S_ν is flux density and ν is frequency. In order to extend the radio frequency coverage and to obtain more accurate radio spectral indices we have also used some flux densities from other radio catalogues; Clarke et al. (1976) at 0.408 GHz, Mills et al. (1984) at 0.843 GHz and Milne et al. (1980) at 14.7 GHz. Spectral indices are not given for 10 LMC and six SMC sources which were detected at only one radio frequency or for which radio data are only available at two close frequencies (4.75 GHz and 4.85 GHz).

Column 8 of Tables 2 and 3 gives the "radio source type" based on published references (Col. 9); these sources are marked with capital letters BG (background sources), H II regions and SNR. In the case of SNRs, where applicable, we have divided the sources into one of five different types: SNR1 to SNR5 respectively (type 1 – evolved SNRs, type 2 – Oxygen-rich SNRs, type 3 – Balmer-dominated SNRs, type 4 – Crab-like SNRs and type 5 – possible type III SNRs). This follows the classification of Mathewson et al. (1983a). Note that capitals (BG, SNR and H II) were used for classifications from previous works and lower case (bg and snr) for sources classified here. The question-mark indicates probable but not certain

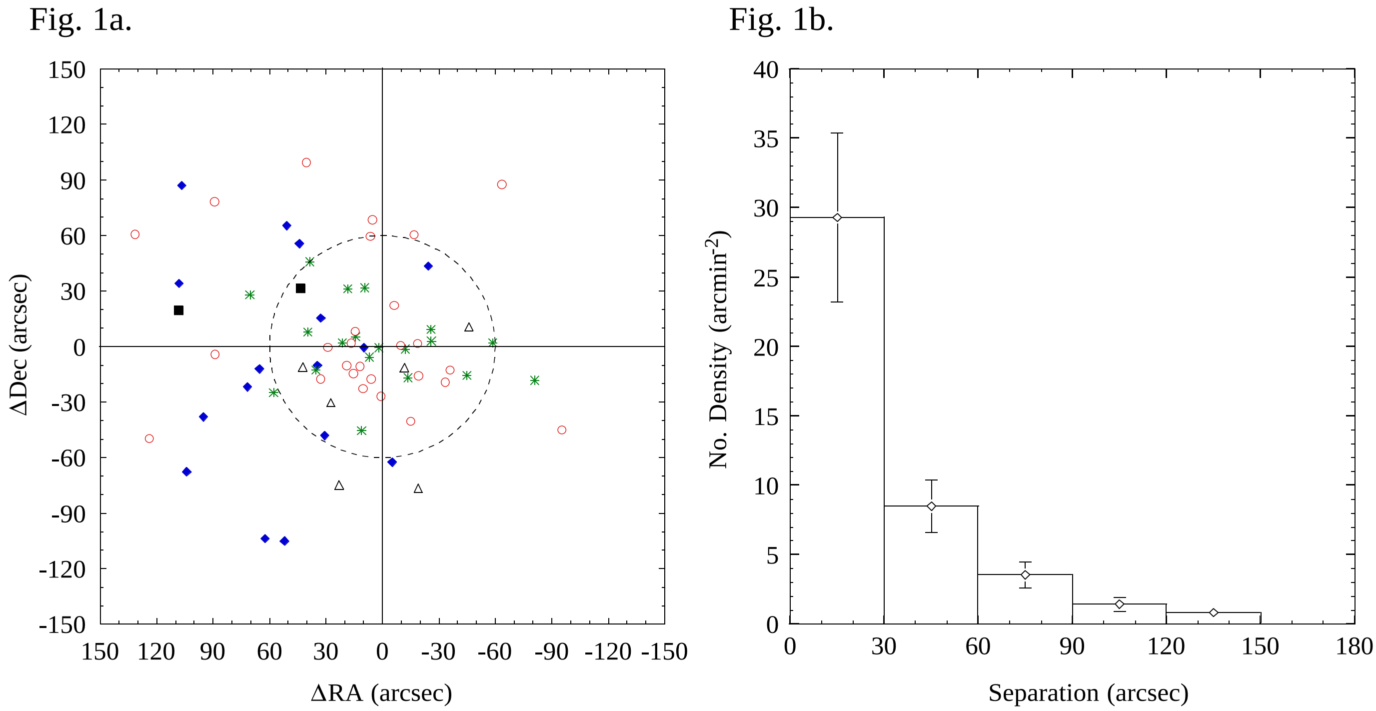

Fig. 1. a) The differences between radio and X-ray source positions for the LMC. Asterisks represents SNRs; filled diamonds – SNRs embedded in H II regions; open circles – background sources; filled square – H II regions and triangles – unclassified sources. Further details are given in Sect. 3.1. The dashed circle is 1′ radius. **b)** The number of sources as a function of radio – X-ray source separation towards the LMC per unit area of the radial bin (per arcmin^2)

classification. The criteria by which we classify these sources are discussed in Sect. 4.1.

A cross-check of all 71 sources towards the LMC and 27 sources towards the SMC has been made with a wide range of catalogues that contain discrete sources towards the MCs (Col. 10). The catalogues used are given as a footnote to Tables 2 and 3. Some comments regarding the discrete sources are given in Col. 11.

3.1. Positional differences for sources in common towards the LMC

The results of the position comparison for all sources common to the Parkes radio and RASS X-ray surveys of the LMC are shown in Figs. 1a and 1b. For the 71 sources, the mean difference in right ascension (RA) is $22'' \pm 6''$ (radio – X-ray) with standard deviation (SD) of $52''$. The difference in declination (Dec) is $0'' \pm 5''$ (SD $= 43''$). Figure 1b shows that there is an excess in the number of sources with small radio – X-ray differences, as expected, well above the number resulting from random coincidence.

Dividing this sample into (i) SNRs, (ii) SNRs embedded in H II regions and (iii) background sources, and again comparing radio – X-ray source positions we obtain: ΔRA $= +5'' \pm 8''$ and ΔDec $= -1'' \pm 5''$ for 19 SNRs; ΔRA $= +63'' \pm 13''$ and ΔDec $= -3'' \pm 15''$ for 17 SNRs embedded in H II regions, and ΔRA $= +12'' \pm 10''$ and

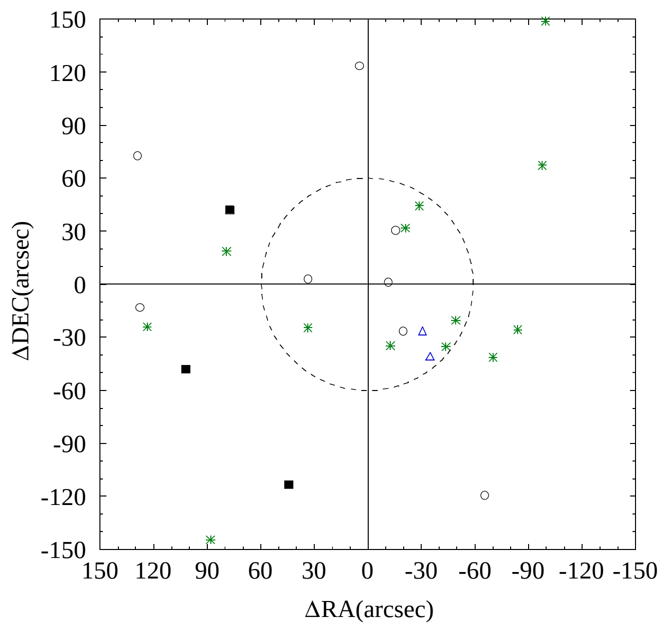

Fig. 2. The differences between radio and X-ray source positions for the SMC. Asterisks represents SNRs; open circles – background sources; filled square – H II regions and triangles – unclassified sources. The dashed circle is 1′ radius

Table 2. Catalogue of the LMC radio sources identified in the RASS. The X-ray source name (Col. 3) is taken from Pietsch et al. (in preparation). More details are given in Sect. 3

(1) No.	(2) Radio Source Name	(3) X-Ray Source Name	(4) $S_{4.75}$ (Jy)	(5) Count Rate cts ks^{-1}	(6) $\alpha \pm \Delta\alpha$	(7) HR 2	(8) Type	(9) References[†]
1	LMC B0428 − 6755	LMC RASS 9001	0.240	4.8	-0.62 ± 0.04	1.00	BG	7; 25
2	LMC B0438 − 7316	LMC RASS 66	0.108	27.4	-0.90 ± 0.05	0.07	bg	
3	LMC B0441 − 6957	LMC RASS 75	0.258	5.2	-0.07 ± 0.21	0.51	bg	
4	LMC B0442 − 6824	LMC RASS 78	0.047	7.7	0.23 ± 0.06	0.28	bg	
5	LMC B0445 − 6458	LMC RASS 84	0.085	59.6	-0.02 ± 0.21	0.07	bg	
6	LMC B0446 − 7210	LMC RASS 9002	0.091	12.1	-0.65 ± 0.04	0.68	bg	
7	LMC B0453 − 6834	LMC RASS 100	0.140	410.1	-0.40 ± 0.09	−0.30	SNR	20; 22; 27
8	LMC B0454 − 6630	LMC RASS 103	0.060	23.7	-0.49 ± 0.05	−1.00	SNR	5; 13; 20; 22; 27; 28
9	LMC B0454 − 6718	LMC RASS 102		37.4		−0.33	SNR	4
10	LMC B0454 − 6806	LMC RASS 9003	0.058	7.2		0.38	?	
11	LMC B0455 − 6843	LMC RASS 104	0.141	16.4	-0.45 ± 0.04	−0.07	SNR	5; 8; 20; 22; 27; 28
12	LMC B0456 − 6803	LMC RASS 106		6.4		0.03	?	
13	LMC B0502 − 6638	LMC RASS 125	0.033	70.9	-2.11 ± 0.11	0.20	BG	
14	LMC B0506 − 6806	LMC RASS 136	0.226	926.7	-0.58 ± 0.06	−0.20	SNR	
15	LMC B0507 − 6829	LMC RASS 141	0.245	5.0	-0.63 ± 0.04	−0.61	SNR?	8
16	LMC B0507 − 7029	LMC RASS 139	0.146	27.1	-0.72 ± 0.05	0.52	SNR?	8
17	LMC B0508 − 6436	LMC RASS 146	0.077	17.3	0.56 ± 0.21	0.14	bg	
18	LMC B0509 − 6848	LMC RASS 149	0.529	1322.7	-0.57 ± 0.11	0.22	SNR4	13; 14; 20; 22; 27; 28
19	LMC B0513 − 6729	LMC RASS 9004	0.186	3.2	-0.48 ± 0.03	1.00	?	
20	LMC B0513 − 6915	LMC RASS 166	0.264	8.7	-0.45 ± 0.16	−0.27	SNR1	23
21	LMC B0519 − 6905	LMC RASS 183	0.072^{f}	1273.1	-0.47 ± 0.14	0.03	SNR3	13; 14; 20; 22; 27; 35
22	LMC B0519 − 6941	LMC RASS 180	0.866	16.2	-0.35 ± 0.04	−0.32	SNR	1; 13; 19; 20; 22; 27; 28; 30
23	LMC B0520 − 6928	LMC RASS 185	0.111	81.9	-0.32 ± 0.05	0.14	SNR	22; 27
24	LMC B0522 − 6757	LMC RASS 192	0.236	89.3	-0.02 ± 0.08	−0.05	SNR	6; 13; 20; 26; 28; 54
25	LMC B0523 − 6623	LMC RASS 9005	0.100	4.5	0.26 ± 0.26	1.00	?	
26	LMC B0524 − 6443	LMC RASS 202	0.043	7.7	-0.78 ± 0.11	0.49	bg	
27	LMC B0525 − 6601	LMC RASS 205	0.390	1010.3	-0.60 ± 0.12	−0.04	SNR5	15; 20; 22; 27; 28; 29
28	LMC B0525 − 6607	LMC RASS 207	1.009	1487.8	-0.51 ± 0.06	0.02	SNR5	1; 5; 9; 13; 15; 22; 27; 28; 36; 50
29	LMC B0525 − 6941	LMC RASS 203	2.251	8764.9	-0.58 ± 0.03	0.02	SNR2	1; 13; 14; 17; 20; 22; 27; 28
30	LMC B0528 − 6542	LMC RASS 9006	0.035	2.2		0.32	?	
31	LMC B0528 − 6551	LMC RASS 213	0.108	12.3	-0.32 ± 0.04	−0.24	SNR	8; 22; 27
32	LMC B0528 − 6838	LMC RASS 214	0.210	18.8		−0.13	snr?	
33	LMC B0528 − 6914	LMC RASS 210	0.075	14.2	-0.44 ± 0.03	−0.05	SNR1	27; 42
34	LMC B0530 − 6655	LMC RASS 220	0.100	15.0	-0.82 ± 0.11	−0.55	snr?	
35	LMC B0531 − 6518	LMC RASS 223	0.041	31.3	0.00 ± 0.11	0.44	bg?	
36	LMC B0532 − 6734	LMC RASS 229	0.093	69.0	-0.56 ± 0.12	−0.35	SNR?	23; 37
37	LMC B0532 − 7102	LMC RASS 225	0.382^{f}	49.6	-0.31 ± 0.02	−0.50	SNR	20; 22; 27
38	LMC B0534 − 6438	LMC RASS 9007	0.058	6.9	-0.59 ± 0.11	0.89	bg	
39	LMC B0534 − 6957	LMC RASS 237	0.054	194.7	-0.48 ± 0.05	−0.28	SNR1	20; 22; 27
40	LMC B0534 − 7035	LMC RASS 239	0.067	31.3	-0.44 ± 0.03	0.06	SNR	20; 22; 24; 27
41	LMC B0534 − 7204	LMC RASS 236	0.103	5.4	-0.32 ± 0.04	−0.89	snr?	
42	LMC B0535 − 6603	LMC RASS 245	0.701	5508.2	-0.57 ± 0.05	0.02	SNR4	1; 9; 10; 13; 15; 22; 27; 28; 33; 39
43	LMC B0536 − 6452	LMC RASS 250	0.050	25.2	-0.77 ± 0.21	0.13	bg	
44	LMC B0536 − 6735	LMC RASS 247	0.133^{f}	49.8	-0.38 ± 0.12	0.37	SNR1	23
45	LMC B0536 − 7040	LMC RASS 248	0.025	39.4	-0.61 ± 0.05	0.40	SNR	20; 22; 24; 27
46	LMC B0537 − 6506	LMC RASS 253	0.035	30.8		0.50	bg?	
47	LMC B0538 − 6911	LMC RASS 254	3.571	142.9	-0.15 ± 0.05	0.55	SNR4	5; 9; 11; 13; 20; 22; 27; 28
48	LMC B0539 − 6907	LMC RASS 9008	35.787	27.4	-0.11 ± 0.02	0.32	H ii	1; 2; 3; 25; 31; 33; 46; 47; 54
49	LMC B0540 − 6921	LMC RASS 265	0.980	579.7	-0.37 ± 0.07	0.54	SNR2	20; 21; 22; 27; 28; 34; 54
50	LMC B0540 − 6946	LMC RASS 264	4.186	7080.5	-0.17 ± 0.01	0.76	H ii	1; 2; 3; 16; 18; 25; 31; 39; 52; 53

(1) No.	(10) Other Names‡	(11) Comments
1	MC 2; MC4(0428-679); PMN J0428 − 6749; PKS B0428 − 679	S_5 from 48 used instead of $S_{4.75}$
2	MC4(0439-732A,B); PMN J0438 − 7310	
3	MC 6; PMN J0440 − 6952	
4	PMN J0442 − 6818	
5		
6	MC4(0446 − 721); PMN J0446 − 7205	
7	MC4(0453 − 685); LHG 1 (W2); PMN J0453 − 6829	Pop II?
8	N11L; DEM L34a	Pop I; S_5 from 28 used instead of $S_{4.75}$
9		
10	PMN J0454-6800	
11	N 86; MC4(0456 − 687); DEM L33; LHG 2 (W3); PMN J0455 − 6838	Pop II?
12		
13	QSO B0502-665	
14	MC4(0506-680); LHG 11 (W10)	Pop I?
15	N 100; DEM L76; PMN J0506 − 6824	
16	DEM L80; NGC 1845; PMN J0506 − 7026; LH26	
17		
18	N 103A,B; MC 22; MC4(0509 − 687A,B); DEM L84(85); LHG 13 (W11); NGC1850; PMN J0508 − 6844; IJL 34	Pop I; SNR embedded in H ii region; Poor positional agreement
19	N 30; MC 25; MC4(0514 − 676); DEM L112(106); NGC 1871; PMN J0513 − 6724; LH38; IJL 41	MC position shifted in RA by 5′ and in DEC by 10′; Star HD 34632 in the field
20	N 112; MC4(0513 − 692A); DEM L109; IJL 39	Pop I?
21	LHG 26 (W24)	Pop II
22	N 120A,B,C; MC 31; MC4(0519 − 696A,B,C); DEM L134; NGC 1918; LHG 23 (W21); IJL 47; LH42; CO 17; PMN J0519 − 6938; PKS B0519 − 696	Pop I; $S_{8.55}$ includes LMC B0518 − 6937; SNR embedded in H ii region; Extended complex of radio sources
23	MC4(0520 − 695); LHG 27 (W25); PMN J0519 − 6926; Sa 113	Pop II?; Poor positional agreement
24	N 44I; MC4(0522 − 679C); DEM L156; LHG 31 (W29); LH48	SNR embedded in H ii region; X-ext; Blended with H ii region N 44B,C (LMC B0522 − 6800)
25	N 46; MC 36; DEM L162; NGC 1941; IJL 56	S_5 from 48 used instead of $S_{4.75}$
26	MC4(0524 − 647)	
27	N 49B; MC 42; MC4(0525 − 660B); DEM L181; LHG 34 (W37)	Pop I
28	N 49A; MC 43; MC4(0525 − 661A); DEM L190; LH53; LHG 36 (W39); PMN J0526 − 6604; PKS B0525 − 661	Pop I
29	N 132D; MC 39; MC4(0525 − 696); DEM L186; LHG 35 (W38); PMN J0525 − 6938; PKS B0525 − 696	Pop I; SNR embedded in H ii region
30		Star HD 271294 in the field
31	MC 48; MC4(0528 − 658); DEM L204; LHG 39; PMN J0528 − 6550	Pop II?; Radio extended; Poor positional agreement
32	W46	Star GSC 9162.0555 is in the field
33	LHG 40 (W42); PMN J0527 − 6911	Pop I; X-ray source consists of two sources: one on soft band (star) and SNR on hard bands
34		
35		Poor positional agreement
36	N 56; MC4(0532 − 675); LHG 48 (W53); NGC 2011; LH75	Poor positional agreement
37	N 206; MC4(0532 − 710B); LHG 47 (W54)	Pop I; SNR embedded in H ii region
38		
39	LHG 53 (W60)	Pop I?
40	MC b; MC4(0534 − 706); DEM L238; LHG 54 (W61); NGC 2038; PMN J0534 − 7034	Pop II?
41	MC4(0534 − 720); PMN J0534 − 7202	Poor positional agreement
42	N 63A; MC 63; MC4(0535 − 660); DEM L243; LHG 59 (W65); NGC 2030; PMN J0535 − 6601; LH83; PKSB0535 − 660; IJL 73	Pop I; SNR embedded in H ii region
43		Star GSC 8887.04000 in the field
44	N 59B; MC4(0536 − 675B); DEM L241; LHG 60 (W67); LH88	Poor positional agreement
45	MC d; MC4(0536 − 706); DEM L249; LHG 61 (W70); NGC 2056; PMN J0535 − 7038	Pop II?
46		AGN; X-var; Galaxy
47	N 157B; MC4(0538-691); LHG 67 (W73); NGC 2060; LH99	Pop I; SNR embedded in H ii region
48	30 Dor; N 157A; MC 74; MC4(0539 − 691); DEM L263; NGC 2070; LHG 72(W72(76,78)); PMN J0538 − 6905; LH100; PKS B0539 − 691	SG(X)
49	N 158A; MC 78; MC4(0540 − 693); DEM L269; LHG 79 (W87); NGC 2081; PSR B0540 − 69; LH104; PKS B0540 − 693	Pop I
50	N 159A; MC 77; MC4(0540 − 697A); DEM L271; LHG 78 (W84); NGC 2079; PMN J0539 − 6944; LH105; CO 33; PKS B0540 − 697; IJL 82	LMC X-1; He iii region; X-var; SNR? X-ray position in RA shifted by 1.5′

(1) No.	(2) Radio Source Name	(3) X-Ray Source Name	(4) $S_{4.75}$ (Jy)	(5) Count Rate cts ks^{-1}	(6) $\alpha \pm \Delta\alpha$	(7) HR 2	(8) Type	(9) References†
51	LMC B0542 − 6702	LMC RASS 275	0.126	6.1	0.30 ± 0.18	−0.57	snr?	
52	LMC B0543 − 7333	LMC RASS 276	0.815	8.1	-0.59 ± 0.06	1.00	BG	1; 25
53	LMC B0544 − 6910	LMC RASS 282		9.2		−0.95	snr?	
54	LMC B0544 − 7030	LMC RASS 283		9.4		−0.05	snr?	
55	LMC B0546 − 6416	LMC RASS 292	0.232^f	231.9	0.28 ± 0.15	0.16	bg	
56	LMC B0547 − 6729	LMC RASS 299	0.087	15.9	0.42 ± 0.07	0.35	bg?	
57	LMC B0547 − 6746	LMC RASS 297	0.063	5.7	-0.58 ± 0.05	0.42	BG	12
58	LMC B0547 − 6942	LMC RASS 296	0.565	36.6	-0.61 ± 0.09	0.24	SNR2	1; 5; 13; 20; 22; 27; 28; 51
59	LMC B0548 − 7025	LMC RASS 298	0.046	116.0	-0.55 ± 0.06	−0.12	SNR3	20; 22; 27; 35
60	LMC B0550 − 6823	LMC RASS 309	0.388	10.9	-0.37 ± 0.06	−0.29	SNR?	1; 25; 32
61	LMC B0552 − 6402	LMC RASS 318	0.154^f	127.3	0.16 ± 0.21	0.15	bg	
62	LMC B0552 − 6948	LMC RASS 320	0.040	32.9	-1.00 ± 0.04	0.36	bg?	
63	LMC B0553 − 6704	LMC RASS 322		2.4		0.54	bg?	
64	LMC B0557 − 6854	LMC RASS 343	0.056	5.0	-0.06 ± 0.08	0.10	?	
65	LMC B0602 − 6443	LMC RASS 378	0.299	3.7	-1.15 ± 0.06	0.01	BG	25; 32
66	LMC B0602 − 6830	LMC RASS 379	0.060	3.5	0.14 ± 0.22	0.01	bg	
67	LMC B0605 − 6625	LMC RASS 390	0.065^f	3.2	-0.81 ± 0.17	0.14	bg	
68	LMC B0606 − 7041	LMC RASS 396	0.052^f	18.5	0.03 ± 0.21	0.51	bg	
69	LMC B0608 − 6510	LMC RASS 409	0.061^f	17.4	-0.88 ± 0.06	0.10	bg	
70	LMC B0611 − 6623	LMC RASS 430	0.210	166.4	-0.69 ± 0.07	0.18	BG	38
71	LMC B0611 − 6734	LMC RASS 429		6.6		0.23	bg	

†References used in Table 2 (Col. 9), Table 4 (Col. 6) and Table 5 (Col. 7).

[1] Bolton & Butler (1975)
[2] Caplan & Deharveng (1986)
[3] Caplan & Deharveng (1985)
[4] Smith et al. (1994)
[5] Chu & Kennicutt (1988a)
[6] Chu et al. (1993)
[7] Corwin et al. (1985)
[8] Davies et al. (1976)
[9] Dennefeld (1982)
[10] Dickel et al. (1993)
[11] Dickel et al. (1994)
[12] Dickey et al. (1994)
[13] Dickel et al. (1994)
[14] Dickel & Milne (1995)
[15] Graham et al. (1987)
[16] Hunt & Whiteoak (1994)
[17] Hwang et al. (1993)
[18] Jones et al. (1986)
[19] Laval et al. (1992)
[20] Long et al. (1981)
[21] Manchester et al. (1993)
[22] Mathewson et al. (1983)
[23] Mathewson et al. (1985)
[24] McGee et al. (1972b)
[25] McGee & Newton (1972)
[26] Meaburn & Laspias (1991)
[27] Mills et al. (1984)
[28] Milne et al. (1980)
[29] Pizzichini et al. (1983)
[30] Rosado et al. (1993a)
[31] Rosa (1993)
[32] Savage (1976)
[33] Shull (1983)
[34] Taylor et al. (1993)
[35] Tuohy et al. (1983)
[36] Vancura et al. (1992)
[37] Wang & Helfand (1991)
[38] White et al. (1987)
[39] Wilcots (1994)
[40] Laustsen et al. (1987)
[41] Laval et al. (1989)
[42] Mathewson et al. (1984)
[43] DeGioia – Eastwood (1992)
[44] Chu et al. (1994)
[45] Chu et al. (1995a)
[46] Chu & Kennicutt (1994)
[47] Wang & Helfand (1991a)
[48] McGee et al. (1972a)
[49] Chu et al. (1995b)
[50] Dickel et al. (1995)
[51] Williams et al. (1997)
[52] Chu et al. (1997).
[53] israel et al. (1996)
[54] Chu & Low (1990)

ΔDec $= +9'' \pm 8''$ for 27 background sources. There are two H II regions and six unclassified sources.

Clearly, there is a large RA positional difference for SNRs embedded in H II, regions and the nature of this difference is the subject of further investigation. Excluding the embedded SNRs and source LMC B0540 − 6946 (LMC X-1; see Sect. 4.6), the positional alignment of the Parkes radio and RASS surveys is good with differences of ΔRA $= +9'' \pm 6''$, ΔDec $= +1'' \pm 5''$ (radio −X − ray), with standard deviations in the differences of $44''$ and $37''$ respectively.

This uncertainty is consistent with the combined positional uncertainties for the radio and the X-ray sources, and retrospectively justifies the initial identification criteria of $2.5'$ (which is equivalent to 3.4σ in RA and 4.1σ in Dec).

3.2. Positional differences for sources in common towards the SMC

We have compared the positions for all 27 sources common to radio and X-ray surveys of the SMC. We used the same criterion for source identification as that used for the LMC survey, i.e., the source must lie within $2.5'$ of its counterpart. This criterion was chosen according to the upper limit of positional uncertainties at our 1.42 GHz survey. These positions were compared with X-ray positions from Kahabka et al. (in preparation).

The results of this comparison are shown in Fig. 2. For the 27 sources, the mean difference in RA is $0'' \pm 15''$ (SD $= 76''$) and in Dec is $-6'' \pm 13''$ (SD $= 66''$). Thus, we have found no significant positional bias between our radio positions and those from the ROSAT PSPC surveys.

(1) No.	(10) Other Names‡	(11) Comments
51		Poor positional agreement
52	MC 83; MC4(0543 − 735); PKS B0542 − 736	AGN
53		
54		
55		X-var; 1ES 0546 − 642; Two Galaxies?
56	NGC 2117; PMN J0547 − 6728	
57	MC4(0547 − 677); W 98; PMN J0547 − 6745	
58	N 135; MC 89; MC4(0547 − 697); DEM L316; LHG 88 (W97); PMN J0547 − 6942; CO 39; PKS B0547 − 697	Pop II; Position for N 135 is not given in Henize (1956); Milne et al. (1980) and Long et al. (1981) identified as N 135
59	LHG 89 (W99); CO 40	Pop II
60	MC 92; MC4(0550 − 683); DEM L328; PMN J0550 − 6822; PKS B0550 − 683	Extended radio source; Poor positional agreement
61	MC4(0550 − 641A); PKS B0551 − 640	
62	MC4(0552 − 698); LHG 93 (W102); PMN J0552 − 6947	
63		
64		
65	MC 94; MC4(0602 − 647); PMN J0602 − 6443; PKS B0602 − 647	Double Galaxy; $S_{8.4}$ from 32 used instead of $S_{8.55}$
66	PMN J0602 − 6830	Star GSC 9164.1193 in the field
67	MC4(0605 − 664)	
68		X-ext; Star GSC 9168.1191 in the field; Galaxy
69	MC4(0608 − 651)	
70	MC4(0611 − 663); PKS B0611 − 663	S_5 from 38 used instead of $S_{4.75}$; Galaxy
71		

‡Abbreviations used in Col. 10.

N	Hα catalogue of emission nebulae (Henize 1956),
MC	Radio catalogue (5.00 GHz) (McGee et al. 1972a),
MC4	Radio catalogue (0.408 GHz) (Clarke et al. 1976),
DEM L	Hα catalogue of emission nebulae (Davies et al. 1976),
NGC	NGC 2000 catalogue (optical) (Sinnott 1988),
LHG	Einstein X-ray catalogue (Long et al. 1981),
W	Einstein X-ray catalogue (Wang et al. 1991),
PSR	Catalogue of pulsars (Taylor et al. 1993),
PMN	Radio catalogue (4.85 GHz) (Wright et al. 1994),
PKS	PKSCAT-90 radio catalogue (Otrupcek & Wright 1991),
Sa	Catalogue of planetary nebula (Sanduleak et al. 1978; Sanduleak 1984),
CO	Catalogue of CO molecular clouds (Cohen et al. 1988),
IJL	Catalogue of CO molecular clouds (Israel et al. 1993) and
LH	Catalogue of stellar associations (Lucke & Hodge 1970).

4. Classification and analysis of discrete sources in common

Out of the 71 sources common to the Parkes radio and RASS surveys of the LMC, 38 have been previously classified (see Table 2, Col. 8). Most are SNRs (30, including four SNR candidates) and background sources (six). Only two X-ray sources from the radio surveys are listed as H II regions. One of them is a chance coincidence with the X-ray binary LMC X-1 (Sect. 4.6) and the other is 30 Doradus.

Out of the 27 sources common to the Parkes radio and the ROSAT PSPC surveys of the SMC, 23 have been previously classified (see Table 3, Col. 8). There are 12 SNRs, seven background sources and three H II regions. One source (SMC B0035 − 7228) appears to be a chance coincidence with the SMC X-ray super-soft source (Sect. 4.3).

Of 52 confirmed radio H II regions in the LMC (Filipović et al. 1997b, hereafter Paper VII), seven sources appear on the Einstein X-ray lists of Helfand et al. (1991), Wang & Helfand (1991b) and Wang et al. (1991). The small number of X-ray emitting H II regions in the RASS LMC point-source list relative to the number seen with the Einstein survey may result from several causes. Some of the Einstein sources are not found as they are below the RASS detection threshold, and others are too extended to be identified as point sources or are located in confused areas. Another possibility is that the improved RASS source positions may exclude the proposed H II regions as the origin of the X-ray source.

H II regions are excellent SN birth places and we expect a number of SNR X-ray sources to be associated with H II regions (Chu & Low 1990). Another process that could explain the appearance of H II regions in X-ray surveys is shock heating by stellar winds inside the H II regions, but Chu et al. (1995b) argue that stellar winds alone could not produce enough X-ray emission. The most extreme example of this is 30 Doradus which is a bright H II region at both radio and X-ray frequencies with no confirmed SNRs (Dickel et al. 1994). We believe, however, that stellar winds, together with embedded SNRs, could be

Table 3. Catalogue of the SMC radio sources identified in the ROSAT PSPC. The X-ray source name (Col. 3) is taken from Kahabka et al. (in prepration). More details are given in Sect. 3

(1) No.	(2) Radio Source Name	(3) X-Ray Source Name	(4) $S_{4.85}$ (Jy)	(5) Count Rate cts ks^{-1}	(6) $\alpha \pm \Delta\alpha$	(7) HR 2	(8) Type	(9) References†
1	SMC B0034 − 7155	RX J0036.9 − 7138	0.078^f	24.60		0.38		20
2	SMC B0035 − 7228	RX J0037.3 − 7214		503.55		−0.95	bg?	15, 20
3	SMC B0037 − 7327	RX J0038.6 − 7310	0.058	31.70	−0.14±0.20	0.39	BG	18, 20
4	SMC B0039 − 7353	RX J0041.0 − 7336	0.102	9.65	0.11±0.14	−0.14	SNR	18, 20
5	SMC B0040 − 7323	RX J0041.9 − 7308	0.083	5.85	−0.68±0.17	0.59	BG	18, 20
6	SMC B0043 − 7321	RX J0045.1 − 7303	0.090	2.92	0.03±0.11	−0.19	H ii	2, 20
7	SMC B0043 − 7330	RX J0045.6 − 7313	0.039	4.19		0.13	snr?	20
8	SMC B0045 − 7255	RX J0047.2 − 7239	0.020	2.11		1.00	BG?	15, 20
9	SMC B0045 − 7324	RX J0047.6 − 7309	0.932	35.10	−0.15±0.18	0.21	SNR	2, 7, 9, 10, 12, 15, 18, 20
10	SMC *B*0046 − 7333	RX J0048.3 − 7319	0.264	3.87	0.11±0.13	0.41	SNR	2, 7, 9, 10, 12, 20
11	SMC B0047 − 7324	RX J0048.9 − 7306	0.099	1.61	−0.14±0.03	−0.21	H ii	2, 20
12	SMC B0047 − 7332	RX J0049.0 − 7314	0.070^f	12.5	0.25±0.06	0.11	SNR	8, 10, 15, 18, 20
13	SMC B0047 − 7343	RX J0049.8 − 7324	0.046	1.40	0.70±0.04	0.68	BG	18, 20
14	SMC B0049 − 7338	RX J0051.0 − 7321	0.046	118.10	−0.06±0.36	−0.26	SNR	7, 8, 10, 15, 18, 20
15	SMC B0049 − 7356	RX J0050.8 − 7341	0.197^f	4.77	0.18±0.20	0.41	BG	18, 20
16	SMC B0051 − 7254	RX J0053.0 − 7239	0.196	0.96	−0.40±0.21	−0.50	SNR	8, 10, 12, 15, 18, 20
17	SMC B0053 − 7227	RX J0055.4 − 7210	0.057	24.70	−0.44±0.12	0.36	BG	15, 18, 20
18	SMC B0054 − 7235	RX J0056.6 − 7220	0.035	1.95	0.49±0.12	0.55	snr?	20
19	SMC B0057 − 7226	RX J0059.5 − 7210	1.633	226.50	−0.15±0.06	−0.08	SNR	2, 3, 9, 13, 15, 18, 19, 20
20	SMC B0058 − 7149	RX J0100.3 − 7133	0.146	7.91	−0.41±0.14	−0.34	SNR	8, 10, 18; 20
21	SMC B0058 − 7228	RX J0100.7 − 7211		23.97		0.33		15, 20
22	SMC B0101 − 7226	RX J0103.2 − 7209	0.125	9.05	−0.09±0.02	0.35	SNR	7, 9, 10, 17, 15, 18, 20
23	SMC B0102 − 7218	RX J0103.9 − 7202	0.411	506.03	−0.33±0.19	−0.11	SNR	1, 2, 4, 7, 9, 10, 15, 18, 20
24	SMC B0103 − 7239	RX J0105.0 − 7223	0.052	42.60	−0.47±0.29	−0.32	SNR	7, 9, 10, 15, 18, 20
25	SMC B0104 − 7226	RX J0105.3 − 7210	0.212^f	18.80		0.07	SNR	20
26	SMC B0110 − 7318	RX J0111.5 − 7302	0.088	3.03	0.04±0.15	0.32	BG	18, 20
27	SMC B0113 − 7334	RX J0114.2 − 7319	0.328^f	2.96	0.28±0.06	0.71	H ii	2, 18, 20

†References used in Table 3 (Col. 9)

[1] Amy (1994)
[2] Caplan et al. (1996)
[3] Davies et al. (1976)
[4] Dopita et al. (1981)
[5] Hodge & Snow (1975)
[6] Jones & McAdam(1992)
[7] Mathewson et al. (1983)
[8] Mathewson et al. (1984)
[9] Mills et al. (1982)
[10] Mills et al. (1984)
[11] Mountfort et al. (1987)
[12] Rosado et al. (1994)
[13] Rosado et al. (1993b)
[14] Savage et al. (1977)
[15] Wang & Wu (1992)
[16] White et al. (1991)
[17] Ye et al. (1995)
[18] Ye (1988)
[19] Ye et al. (1991)
[20] Kahabka et al. (in preparation).

sufficient for X-ray emission from large H ii regions. Arthur & Henney (1996) proposed a model in which an SNR evolves inside an extremely diffuse stellar-wind bubble (formed by the OB association stars) but the density in the SNR is augmented through hydrodynamic ablation of cool, dense clumps by the post-blast SNR flow.

Most SNRs in the MCs are embedded in H ii regions; 16 such objects have been found. Chu & Kennicutt (1988b) predicted that more embedded SNRs will be identified in future radio surveys of higher angular resolution and sensitivity. These SNRs are rather weak emitters of very small size ($< 5''$) and are obscured within much stronger H ii regions such that their detection is difficult with the present radio survey data.

By comparison, the discovery of further young and luminous SNRs in the MCs isolated from H ii regions in significant numbers is not likely (Clarke 1976). This conjecture is supported by our $\mathrm{Log}N - \mathrm{Log}\,S$ study (Paper VII) where we predict that only a small fraction of our unclassified sources can be SNRs.

4.1. Source classification criteria

To establish a criterion for the classification of the 33 "unknown" LMC and five "unknown" SMC sources and to check the "known" sources, we plot in Figs. 3a and 3b the source radio spectral index against the X-ray HR2. These colour-colour diagrams show several important trends.

First, all known background sources have positive HR2, with mean value for the ones towards the LMC of $\mathrm{HR2_{mean}} = 0.31$ and SD = 0.22 (see Fig. 4b), compared to the HR2 for the LMC SNRs (see Fig. 4a), which have a much wider distribution ($-1.00 < \mathrm{HR2} < 0.55$). All sources with negative HR2 are SNRs or SNR candidates.

(1) No.	(10) Other Names‡	(11) Comments
1		X-ray binary candidate
2	1E0035.4-7230; WW 13	124″ from SMC X-ray Binary; X-ray super-soft source
3	PMN J0038 − 7310	X-ray binary candidate
4	PMN J0040 − 7337; DEM S5; LI-SMC 10	
5	MC4 B0040 − 733A; PMN J0042 − 7306	
6	N 12B; NGC 249; DEM S18; LI-SMC 30	BG in X-ray classification
7	N 10; PMN J0044 − 7313; DEM S11 (14); LI-SMC 28	
8	PMN J0047 − 7239; WW 19; LI-SMC 40	
9	N 19; S9; MC4 B0045 − 734; PMN J0047 − 7308; NGC 261; DEM S32; IKT 2; LI-SMC 43; WW 16; BKGS 1A	SNR embeded in H ii region
10	N 22 (20, 21, 23, 28, 28A); S10; MC4 B0046-735; DEM S37 (36); LI-SMC 45 (42)	SNR embeded in H ii region
11	N 30; S13; DEM S45	
12	DEM S49; IKT 5; WW 22; BKGS 2; LI-SMC 54	
c 13	N 31 (33); PMN J0049 − 7326; DEM S44; LI-SMC 57 (56)	
14	PMN J0051-7321; 1E0049.4 − 7339; IKT 6; WW 24; LI-SMC 68	
15		
16	N 50; DEM S68; PMN J0053 − 7238; WW 30; BKGS 5	
17	MC4 B0053 − 724; PMN J0055 − 7210; NGC 306; WW 36	Two sources in MOST
18	N 58 (57); PMN J0056 − 7219; DEM S86; LI-SMC 110 (109)	
19	N 66 (66A,B,C,D); S17; PKS B0057 − 724; MC4 B0057 − 724; PMN J0059 − 7210; NGC 346; DEM S103; 1E0057.6 − 7228; IKT 18; LI-SMC 131; WW 44	SNR embbedded in H ii region; Emission nebula
20	MC4 B0058 − 718B; PMN J0100 − 7133; DEM S108	
21	1E0059.0 − 7228; IKT 19; WW 45	X-ray binary candidate
22	N 76C; 1E0101.5 − 7226; IKT 21; WW 50; LI-SMC 160	
23	N 76 (76A); S20; PKS B0102 − 723; MC4 B0102 − 723; PMN J0103 − 7202; DEM S124 (123); 1E0102.2 − 7219; IKT 22; WW 51; BKGS 12; LI-SMC 162 (161)	SNR embeded in H ii region; An Oxygen-Rich Young SNR
24	DEM S125; 1E0103.3 − 7240; IKT 23; WW 52; BKGS 13; LI-SMC 169	
25	DEM S128; IKT 24; WW 53; BKGS 14; LI-SMC 170	
26	PMN J0111-7302	
27	N 84; S26; PKS B0113 − 735; MC4 B0112 − 736; NGC 456; PMN J0114 − 7318; DEM S150 (152); LI-SMC 202 (201)	Vicinity of BG source

‡Abbreviations used in Col. 10.

N	Hα catalogue of emission nebulae (Henize 1956),
S	Radio catalogue (McGee et al. 1976),
MC4	Radio catalogue (408 MHz) (Clarke et al. 1976),
MRC	Radio catalogue (408 MHz) (Large et al. 1981),
DEM S	Hα catalogue of emission nebulae (Davies et al. 1976),
NGC	NGC 2000 catalogue (optical) (Sinnott 1988),
PMN	Radio catalogue (4.85 GHz) (Wright et al. 1994),
PKS	PKSCAT-90 radio catalogue (Otrupcek & Wright 1991),
1E	X-ray catalogue (Seward & Mitchell 1981),
IKT	X-ray catalogue (Inoue et al. 1983),
LI − SMC	IR catalogue (Schwering & Israel 1991; Israel et al. 1993),
WW	X-ray catalogue (Wang & Wu 1992) and
BKGS	X-ray catalogue (Bruhweiler et al. (1987).

Second, the LMC SNRs have a narrower range of radio spectral index ($\alpha_{\rm mean} = -0.44$, SD = 0.20; see Fig. 5a) than background sources in the field of the LMC ($\alpha_{\rm mean} = -0.39$, SD = 0.60; see Fig. 5b).

Third, the background sources have two peaks of spectral index: one with very steep radio spectra consisting of 12 sources with $\alpha_{\rm mean} = -0.77$ and SD = 0.19, and another with flat and inverted spectra (10 sources) with $\alpha_{\rm mean} = 0.19$ and SD = 0.24.

Because of the overlap in radio spectral index (Paper VII), spectral index alone is not sufficient to distinguish SNRs, H ii regions and background sources. As an additional help in source classification, we will treat all sources outside the region defined by RA(B1950) $= 04^{\rm h}45^{\rm m}$ to RA(B1950) $= 06^{\rm h}00^{\rm m}$ and Dec(B1950) $= -65°$ to Dec(B1950) $= -72°30'$ as background sources. Also, all sources outside the area of the SMC defined by RA(B1950) $= 00^{\rm h}30^{\rm m}$ to RA(B1950) $= 01^{\rm h}30^{\rm m}$ and Dec(B1950) $= -71°40'$ to Dec(B1950) $= -74°00'$ will be treated as background. No radio sources in these surrounding areas are known to belong to either the LMC or the SMC.

Because of the small number of H ii regions observed in previous X-ray surveys (4 out of 174, Paper VII), we do not believe that any of the previously unclassified (both radio and X-ray) sources in the field of the MCs are compact H ii regions.

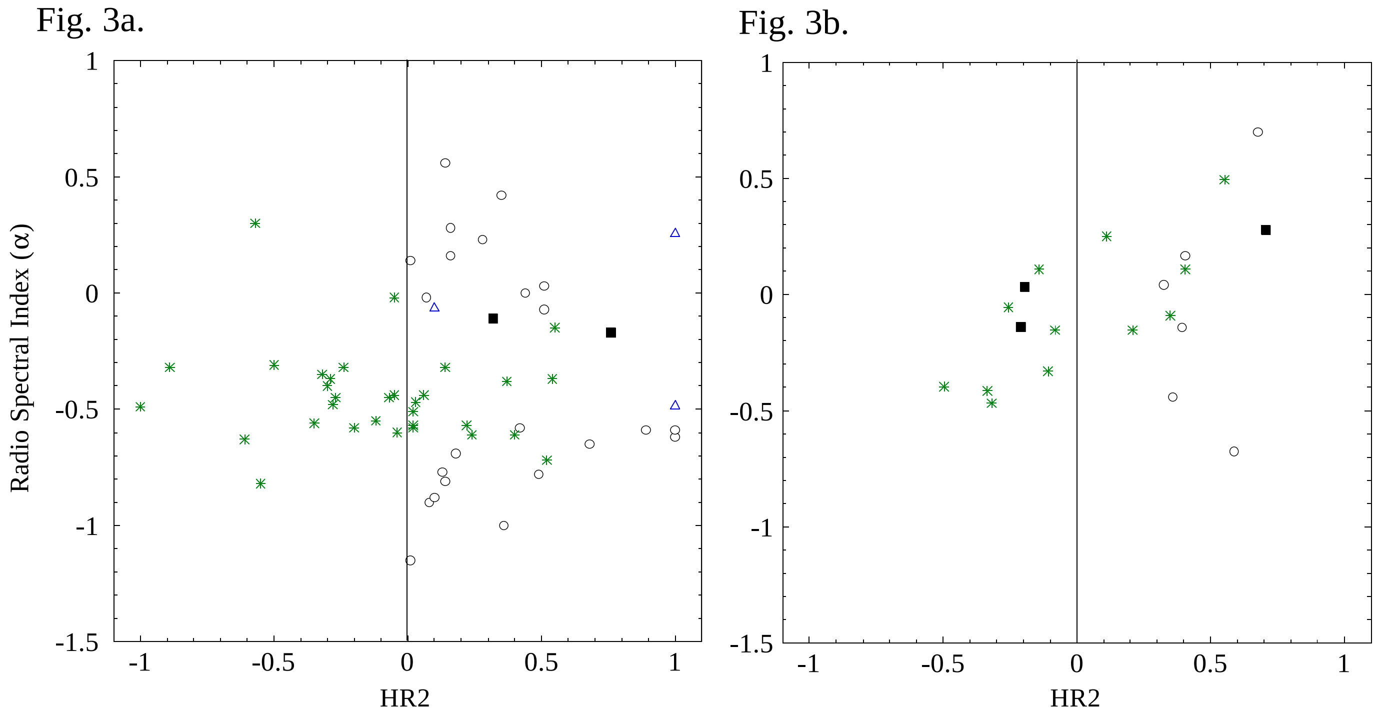

Fig. 3. The distribution of radio spectral index (α) and X-ray hardness ratio 2 (HR2) for different classes of sources towards **a)** the LMC and **b)** the SMC. Asterisks represents SNRs; filled square – H II regions; open circles – background sources and triangles – unclassified sources. All background sources have HR2 > 0

4.2. Background sources in the field of the LMC

A list of background sources towards the LMC is presented in Paper VII. From this list, six known background sources have been confirmed as X-ray emitters: LMC B0428−6755, LMC B0502−6638, LMC B0543−7333, LMC B0547 − 6746, LMC B0602 − 6443 and LMC B0611 − 6623 (see in Table 2, Col. 8 marked with "BG").

There are 16 sources outside the LMC area defined in Sect. 4.1. All of the sources (LMC B0438−7316, LMC B0441−6957, LMC B0442−6824, LMC B0445−6458, LMC B0446−7210, LMC B0508−6436, LMC B0524−6443, LMC B0534−6438, LMC B0536−6452, LMC B0546−6416, LMC B0552−6402, LMC B0602−6830, LMC B0605−6625, LMC B0606 − 7041, LMC B0608 − 6510 and LMC B0611 − 6734) have a positive HR2 and radio spectrum typical of background sources. Here we suggest that all of these sources are background objects (see Table 2, Col. 8 marked with "bg").

Another five sources within the LMC area (LMC B0531−6518, LMC B0537−6506, LMC B0547−6729, LMC B0552−6948 and LMC B0553−6704) are classified as probable background sources because of their positive hardness ratios and/or radio spectra. This classification is strongly based on the HR2 because, as the radio spectra could not be estimated for some of these sources, they were detected at only one radio frequency. These sources are marked in Table 2, Col. 8, with "bg?".

To conclude, 27 out of 71 sources in common towards the LMC appear to be background (or candidates for background) sources. This is consistent with the number expected from Log N − Log S studies of such objects (Paper VII).

4.3. Background sources in the field of the SMC

A catalogue of background radio sources towards the SMC can be found in Paper VII. From this list we found six radio sources (SMC B0037−7327; SMC B0040−7323; SMC B0047−7343; SMC B0049−7356; SMC B0053−7227 and SMC B0110−7318) that are common to the ROSAT PSPC list of sources (Kahabka et al. in preparation). These sources were marked with "BG" in Table 3, Col. 8.

Another radio source (SMC B0045−7255) listed in Paper VII as a background candidate (see in Table 3, Col. 8 marked with "BG?") was found in the ROSAT PSPC X-ray surveys (RX J0047.2 − 7239). This source, with positive HR2, will be treated as a definite background object in future studies.

The X-ray super-soft source RX J0037.3 − 7214 lies $126''$ from the radio source SMC B0035 − 7228 and therefore they are most probably a chance coincidence. We believe that the radio source is likely to be a background object.

In total, 8 out of 27 sources in common towards the SMC appear to be background objects. Seven of them have an X-ray counterpart and one is probably a chance coincidence.

4.4. Supernova remnants in the LMC

Previous studies investigated 56 SNRs in the LMC, from which 37 are confirmed and 18 are candidates (Mathewson et al. 1983, 1984, 1985; Mills et al. 1984; Chu & Kennicutt 1988a, b, 1994; Chu et al. 1993, 1995a, b, 1997;

Fig. 4a.

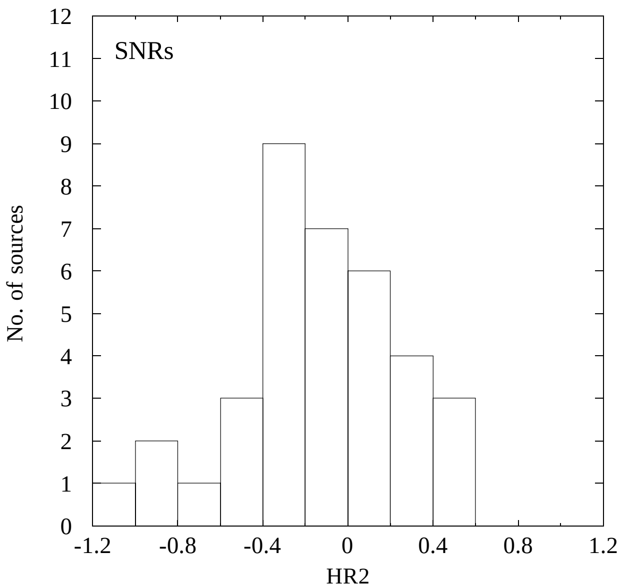

Fig. 4b.

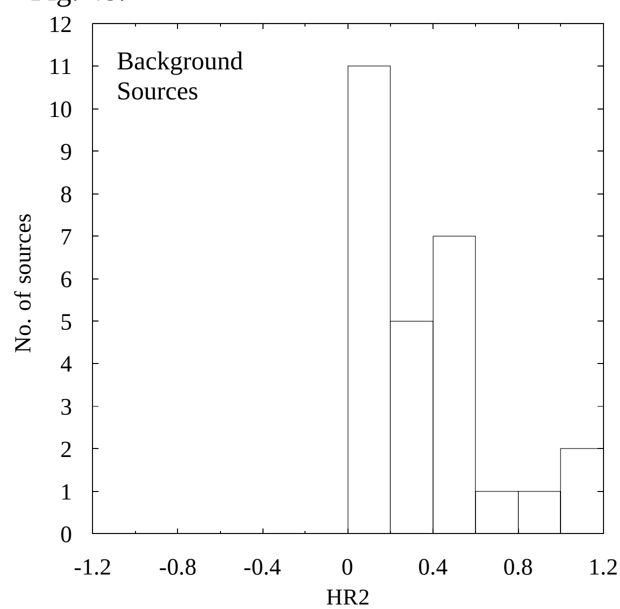

Fig. 4. Distribution of HR2 for **a)** the LMC SNRs, and **b)** background sources towards the LMC

Fig. 5a.

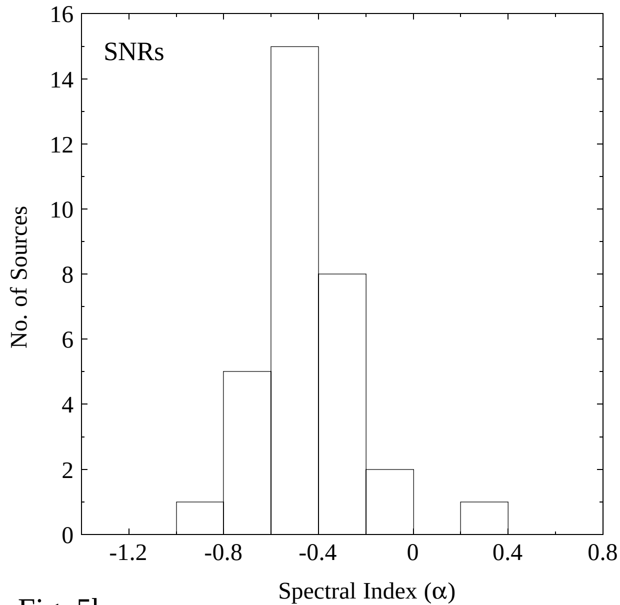

Fig. 5b.

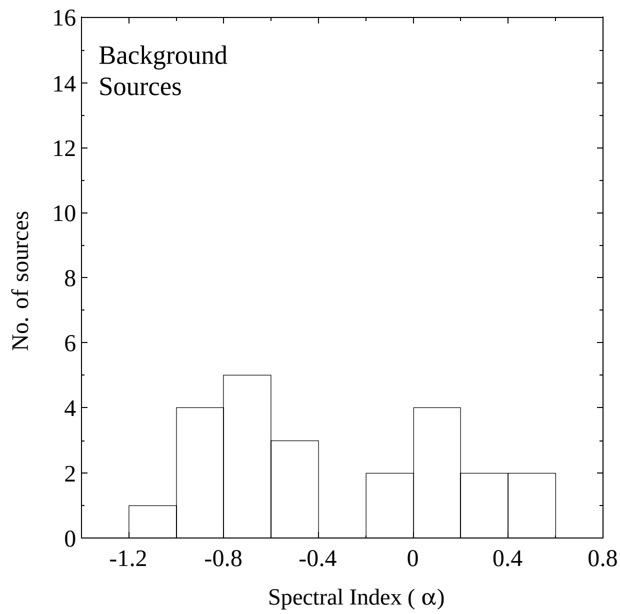

Fig. 5. Distribution of radio spectral index for **a)** the LMC SNRs, and **b)** background sources towards the LMC common to the RASS

Smith et al. 1994; Dickel et al. 1993, 1994; Dickel & Milne 1995). All are detected at radio frequencies. Three confirmed SNRs (B0505 – 679, B0509 – 675 and B0543 – 689) listed in Mathewson et al. (1983a), Mills et al. (1984) and Tuohy et al. (1982) could not be detected in any of the six Parkes radio surveys (their emission is below our detection limits). They were, however, detected at 843 MHz with the Molonglo Observatory Synthesis Telescope (MOST) (Mills et al. 1984). Positive X-ray detection of these three

SNRs has been reported by Wang et al. (1991) and Pietsch et al. (in preparation). Another SNR discovered by Chu et al. (1997) is associated with H II region N159 and we discuss this source in Sect. 4.6.

We have detected 26 SNRs and four SNR candidates in both the X-ray and our Parkes radio surveys. All 30 sources: namely LMC B0453−6834, LMC B0454−6630, LMC B0454−6718, LMC B0455−6843, LMC B0506−6806, LMC B0507−6829, LMC B0507−7029, LMC B0509−6848, LMC B0513−6915, LMC B0519−6905, LMC B0519−6941, LMC B0520−6928, LMC B0522−6757, LMC B0525−6601, LMC B0525−6607, LMC B0525−6941, LMC B0528−6551, LMC B0528−6914, LMC B0530−6734, LMC B0532−7102, LMC B0534−6957, LMC B0534−7035, LMC B0535−6603, LMC B0536−6735, LMC B0536−7040, LMC B0538−6911, LMC B0540−6921, LMC B0547−6942, LMC B0548−7025 and LMC B0550−6823, show strong evidence for being SNRs based on radio spectral index or X-ray HR2, or both. These sources are marked in Table 2, Col. 8 with "SNR" or "SNR?".

Two previously unclassified radio sources (LMC B0530 − 6655 and LMC B0534 − 7204) are strong candidates for being SNRs because of a negative HR2 and steep radio spectral index.

There are another four previously unclassified radio sources (LMC B0528 − 6838, LMC B0542 − 6702, LMC B0544 − 6910, LMC B0544 − 7030) which have a negative HR2, but we have no radio spectral index data, since they are observed only at one radio frequency. These are more likely to be SNRs than background sources and therefore we consider them as SNR candidates (see in Table 2, Col. 8 marked with "snr?").

Thirty SNRs and six new SNR candidates from this study have been classified out of the total number of 71 sources. This increases the total number of SNR candidates known in the LMC from 18 to 24.

4.4.1. Statistics of the LMC supernova remnants

Wang et al. (1991) detected 28 X-ray SNRs from the Einstein survey of the LMC and Smith et al. (1994) and Chu et al. (1995a, 1997) found another seven SNRs from the ROSAT PSPC survey. Here we confirm the existence at X-ray frequencies of an additional five previously known radio SNRs and suggest a further six new SNR candidates. This brings the total number of X-ray SNRs and SNR candidates in the LMC to 46. As the total number of known SNRs and SNR candidates in the LMC is 62, 74% are now confirmed as X-ray sources.

There are four known SNRs and 12 SNR candidates in our Parkes radio surveys for which there are no X-ray counterparts (Table 4). Table 4 contains SNRs drawn from different age populations. There are both strong and weak radio SNRs in Table 4 and so the non-detections in X-rays are not simply because the SNRs are radio weak. The speculation by Aschenbach (1995) for the existence of X-ray quiet SNRs is supported.

It is interesting to note that 33% (60 out of 182), or 48% (89 out of 182 if 29 SNR candidates are included) of the radio SNRs in our Galaxy have been seen in X-ray surveys (Aschenbach 1995). These percentages for our Galaxy are far smaller than for the LMC. The reason may be that soft X-ray emission from some of the Galactic SNRs may be absorbed by H I in the Galactic Plane, whereas X-ray emission from the LMC is less absorbed because of lower column-depths towards the MCs.

4.4.2. An estimate of the supernova rate in the LMC

An estimate of the rate of supernova formation can be obtained if the age of the individual SNRs can be determined. To estimate the age of individual SNRs in the MCs, we follow the method of Van Buren & Greenhouse (1994) and adopt the relationship between age and radio flux density at 4.75 GHz ($S_{4.75}$). For calibration, we have scaled the flux density of Cas A ($S_{4.75} = 650$ Jy) at its distance of 3 kpc, and age of 340 years (Whithfield 1957), to the distance of the LMC (50 kpc; Westerlund 1993) to give the relationship:

$$S_{4.75} = 3887 \times T^{-1.3}$$

where T is the SNR age in years and $S_{4.75}$ is in Jansky (Jy).

Assuming the $S_{4.75}$ flux densities to be complete down to ~ 0.1 Jy (which corresponds to a SNR age of 3400 yr), we have computed the age of 38 SNRs and SNR candidates. It has been assumed that the flux densities are not seriously affected by any confusing H II regions. A comparison of our estimates of the individual SNR ages with diameters taken from various optical and high-resolution radio images shows little correlation and, therefore, we assign little confidence to the individual ages. The mean period between successive SNR occurrences is 100 ($\pm$20) yr. This figure does not agree with the estimate of Chu & Kennicutt (1988b) who give the birth-rate in the LMC of one SNR per 500 yr. However, Chu & Kennicutt (1988b) predict that their estimate of the rate will change with the discovery of new SNRs hidden in H II regions and superbubbles.

Using the radio supernova rate and the relation between star-formation rate (SFR) and supernova rate (Condon 1992; Eq. (20)) it is possible to determine the SFR in the LMC. We obtain an SFR of $0.7(\pm0.2)$ $M_\odot\,\mathrm{yr}^{-1}$. This result is consistant, albeit slightly higher than the upper limit of ~ 0.6 $M_\odot\,\mathrm{yr}^{-1}$ suggested by Kennicutt (1991).

Our estimate of supernova birth-rate in the LMC seems large in comparison to the rate in our Galaxy (one every 30 − 50 yr). Probably, the problem lies in the Van Buren & Greenhouse (1994) relationship which is too simplistic given the poor correlation between ages and flux for

Table 4. Radio SNRs and SNR candidates in the LMC that are not detected with X-ray surveys (RASS or Einstein survey). The references in Col. 5 are the same as in Table 2

(1) Radio Source Name	(2) $S_{4.75}$ (Jy)	(3) $\alpha \pm \Delta\alpha$	(4) Type	(5) Reference	(6) Comments
LMC B0450 − 6927	0.267	-0.68 ± 0.16	SNR?	8; 31	He III region
LMC B0450 − 7055	0.496	-0.36 ± 0.08	SNR1	23; 25	Pop II?
LMC B0454 − 7005	0.166	-0.67 ± 0.09	SNR?	8; 20	
LMC B0459 − 6612			SNR?	8	Seen only at 2.45 GHz
LMC B0505 − 6548	0.046	-1.27 ± 0.21	SNR?	8	
LMC B0520 − 6531	0.505	-0.37 ± 0.15	SNR?	8; 49	X-ray – Superbubble
LMC B0521 − 6545	0.141	-0.33 ± 0.03	SNR?	8; 20	
LMC B0523 − 7138	0.176	-0.86 ± 0.05	SNR?	8; 20	Superbubble
LMC B0524 − 6627	0.050^f	-0.33 ± 0.06	SNR1	20; 23	Pop I; SNR embedded in H II region
LMC B0524 − 7121	0.104	-0.48 ± 0.14	SNR?	8	
LMC B0528 − 6716	0.149	-0.79 ± 0.15	SNR	23	
LMC B0528 − 7038	0.244	0.00 ± 0.02	SNR?	8	
LMC B0529 − 6702	0.208	-0.93 ± 0.06	SNR?	34	Vicinity of Pulsar PSR B0529 − 66
LMC B0537 − 6641	0.442	-0.01 ± 0.12	SNR?	8	
LMC B0538 − 6922	1.012	0.03 ± 0.10	SNR	27; 42	Pop I; SNR embedded in H II region
LMC B0544 − 6621	0.092	-1.34 ± 0.33	SNR?	8	

well-known SNRs. Also, Condon's (1992) relation between SFR (in $M_\odot\,\mathrm{yr}^{-1}$) and SN rate assumes some kind of universal initial mass function (IMF), while we have strong indications for bimodal mass function in the MCs, with the large star masses (hence SNs) strongly favoured in clusters and associations (Massey et al. 1995).

4.5. Supernova remnants in the SMC

From the list of 20 SMC SNRs and SNR candidates (Ye 1988), 12 were found in our Parkes radio surveys (Paper VII). Five well-known SNRs and three SNRs candidates could not be detected in any of our radio surveys but they can all be detected with the MOST radio telescope and are also in the ROSAT PSPC surveys.

All 12 radio SMC SNRs from the Parkes surveys have counterparts in the ROSAT PSPC survey. These 12 sources are: SMC B0039−7353, SMC B0045−7324, SMC B0046−7333, SMC B0047−7332, SMC B0049−7338, SMC B0051−7254, SMC B0057−7226, SMC B0058−7149, SMC B0101−7226, SMC B0102−7218, SMC B0103−7239 and SMC B0104−7226. They show typical SNR characteristics and here we confirm their SNR nature.

Radio sources SMC B0043−7330 and SMC B0054−7235 have not been classified before and we found counterparts in X-ray sources RX J0045.6 − 7313 and RX J0056.6 − 7220. These sources were also detected in Hα and IR surveys and therefore we believe that they could be good SNR candidates. However, neither of these sources has a conclusive radio spectral index or HR2.

4.5.1. An estimate of the supernova rate in the SMC

Using the same method as for the LMC, we estimate the birth-rate of SNRs and the SFR in the SMC. From 12 SMC SNRs, 10 have radio flux at 4.85 GHz greater than 0.1 Jy, which is our completeness level. Using an estimated age of these 10 SMC SNRs, we find that the birth-rate of the SNRs in the SMC is one every 350 ($\pm$70) yr. As for the LMC, this figure does not agree with the previously published estimate of Mathewson et al. (1983) who give the birth-rate in the SMC of one SNR per 800 yr.

Using this birth-rate we obtain an SFR for the SMC of 0.15 ($\pm$0.05) $M_\odot\,\mathrm{yr}^{-1}$. This result is also consistent with the upper limit of $\sim 0.1\ M_\odot\,\mathrm{yr}^{-1}$ suggested by Kennicutt (1991).

4.6. Other MCs sources found in this study

Only five radio H II regions (LMC B0539−6907 = 30 Dor, LMC B0540−6946, SMC B0043−7321; SMC B0047−7324 and SMC B0113−7334) are correlated with X-ray sources in this study. The X-ray emission from the well-known radio H II region(s) LMC B0540 − 6946 (N 159; Hunt & Whiteoak 1994) is caused by the X-ray binary (LMC X − 1) and is therefore not associated with the H II region. Chu et al. (1997) found X-ray emission from N 159A (2′ east of LMC X-1) in the ROSAT HRI image, which they interpret as being coused by an SNR. However, Hunt & Whiteoak (1994) did not find any evidence of such

Table 5. Sources in the field of the LMC detected at radio and X-ray frequencies but not listed in Table 2. These sources are either in the X-ray surveys (RASS, PSPC or Einstein) but not in the Parkes surveys, or in the Parkes surveys but not in the RASS

(1) Radio Source Name	(2) X-ray Source Name	(3) $\alpha \pm \Delta\alpha$	(4) Type	(5) Reference†	(6) Comments
LMC B0453 − 6700	RX J04531 − 6655	-0.55 ± 0.08	SNR	4	
LMC B0500 − 7014	LHG 7; W 7	-0.73 ± 0.19	SNR1	15; 20; 27; 28; 40; 41	Pop I; SNR embedded in H II region
LMC B0501 − 6629	RX J0502 − 6624	-1.27 ± 0.08	SNR?	28	Vicinity of PSR B0502 − 66?
B0505 − 679	LMC RASS 135; LHG 10; W 9	-0.50	SNR3	22; 27; 35	
B0509 − 675	LMC RASS 152; LHG 14; W 12	-0.48	SNR3	27; 35	
LMC B0509 − 6720	RX J0509 − 6717	-0.76 ± 0.04	SNR?	7; 17	
LMC B0517 − 7151	W 18	-0.38 ± 0.07	BG	1; 12	
LMC B0522 − 6800	W 30	-0.48 ± 0.08	H II	2; 3; 6; 13; 26; 28; 31	Near a non-thermal source; He III region
LMC B0523 − 6806	W 31	-0.04 ± 0.06	H II	2; 3; 6; 13; 26; 28	
LMC B0526 − 6731	W 40	-0.27 ± 0.10	H II	2; 3	SB(X)
LMC B0532 − 6743	W 51	-0.01 ± 0.18	H II	2; 3; 28; 43; 44; 54	Curved radio spectrum; Diffuse emission
LMC B0535 − 6948	LHG 56; W 63	0.12 ± 0.05	H II	3; 37; 54	
LMC B0536 − 6914	LHG 62; W 71; RX J05362 − 6911	0.05 ± 0.05	SNR	5; 27	Pop I; SB(X); SNR embedded in H II region
LMC B0536 − 6920	W 66		SNR	45	Seen only at 8.55 GHz
LMC B0539 − 6606	LHG 75	-0.73 ± 0.21			
LMC B0540 − 6927	RX J05402 − 6928				Seen only at 8.55 GHz
B0543 − 689	LMC RASS 278; LHG 82; W 91	-0.29	SNR	27	

†The numbers in this column refer to references given at the end of Table 2.

an SNR in the high-resoulution (∼10″) ATCA radio observations.

There are six sources towards the LMC (LMC B0456−6803, LMC B0454−6806, LMC B0513−6729, LMC B0523 − 6623, LMC B0528 − 6542 and LMC B0557 − 6854) and two towards the SMC (SMC B0034−7155 and SMC B0058−7228) that could be either SNR candidates or background objects with flat radio spectra and positive HR2 close to zero. The classification of these sources, however, remains ambiguous.

There are four foreground stars in the field of the RASS (Pietsch et al. in preparation) that coincide with our radio sources (LMC B0513−6729, LMC B0528−6542, LMC B0528−6838 and LMC B0536−6452). We believe that source LMC B0536−6452 is a background source (Sect. 4.2). We classified the source LMC B0528−6838 as an SNR candidate (Sect. 4.4) and the classification of the remaining two sources (LMC B0513−6729 and LMC B0528−6542) is ambiguous. All of these sources belong to the group of expected random coincidences (see Sect. 3).

4.7. Radio and X-ray sources towards the LMC common to other surveys

So far we have discussed sources detected in the Parkes radio surveys (Papers IV, IVa and V) and the ROSAT X-ray surveys (Pietsch et al. in preparation; Kahabka et al. in preparation). However, there are other sources towards the LMC detected in both radio and X-ray from other surveys which are not listed in Table 2. There are no such sources in the field of the SMC.

In Table 5 we list an additional 14 sources towards the LMC which have been catalogued in Papers IV and IVa but which have not been detected in the RASS. These sources have been detected at X-ray wavelengths by the Einstein surveys by Long et al. (1981) and Wang et al. (1991), and with the ROSAT PSPC by Trümper et al. (1991). Also, we add three confirmed radio SNRs (B0505 − 679, B0509 − 675 and B0543 − 689 detected with the MOST and discussed in Sect. 4.4) which are listed in the RASS but not seen in our radio surveys (Table 5).

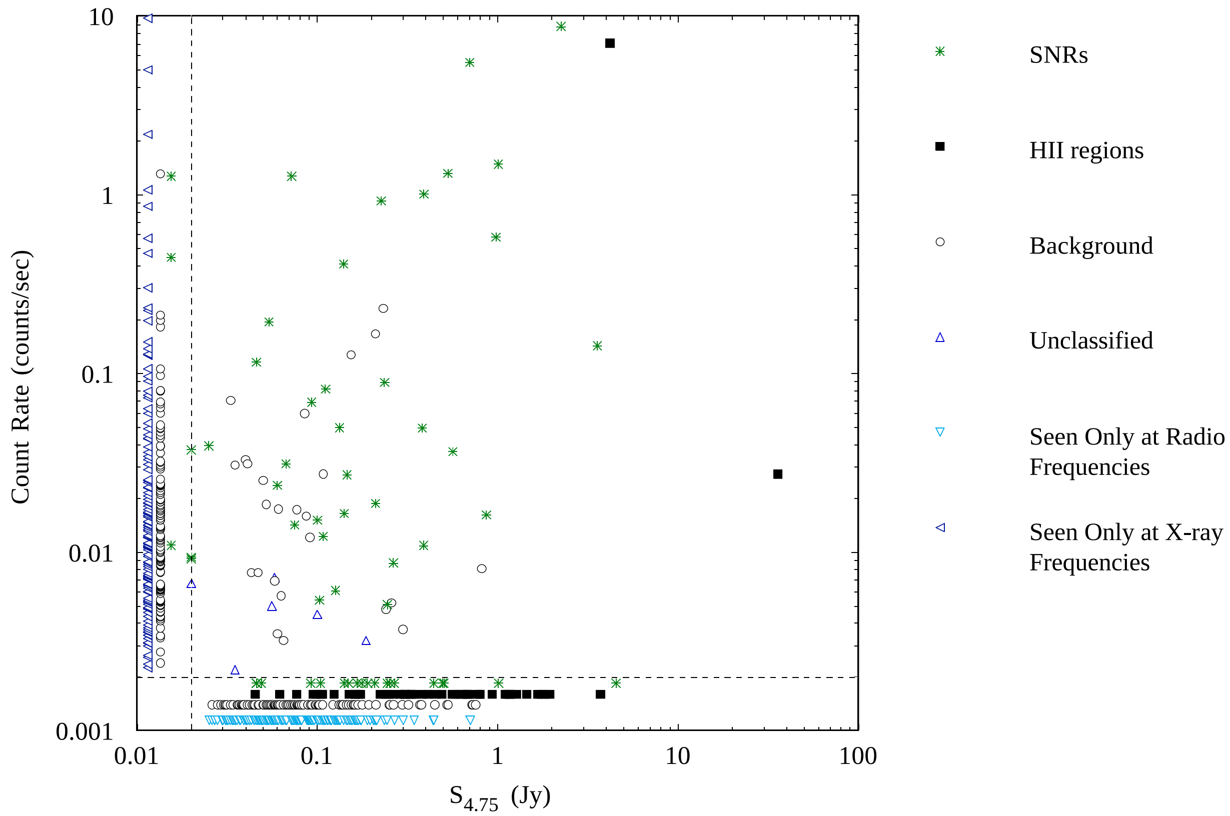

Fig. 6. The distribution of X-ray count rate and radio flux density at 4.75 GHz for different classes of sources in the LMC. Asterisks represents SNRs; filled squares – H II regions; open circles – background sources and open triangles – unclassified sources. The dashed lines represent the approximate threshold in radio and X-ray surveys. Sources below the dashed lines represent non-detections

All abbreviations and lists of references in Table 5 are based on the nomenclature used in Table 2, with the exception of the X-ray information (count rate and HR2).

Of these 17 sources, nine are known SNRs, five are H II regions and one is a known background source (see Table 5, Col. 4). The classification of sources LMC B0539 – 6606 and LMC B0540 – 6927 is ambiguous but they are likely to be SNR candidates.

5. Radio to X-ray source intensity comparison

In Fig. 6 we have compared the X-ray source intensity (count rate, Table 2, Col. 5) from the RASS with the radio flux density from the 4.75 GHz LMC survey (Table 2, Col. 4). A similar comparison for the SMC is shown in Fig. 7 where we compared the source radio flux from 4.85 GHz survey (Table 3, Col. 4) with the X-ray source intensity (count rate, Table 3, Col. 5) from the ROSAT SMC PSPC surveys.

Most of the radio sources in the field of the LMC (412 out of 483; 85%) fall below the sensitivity limit of the RASS survey (shown in Fig. 6 below 0.002 counts s^{-1}) while most of the X-ray sources (254 out of 325; 78%) fall below the sensitivity limit of the radio survey (shown below 0.2 Jy). Many strong radio sources and strong X-ray sources have not been detected at X-ray and radio frequencies, respectively. For the SNRs embedded in H II regions, a small component of the radio flux will be caused by the H II regions but this will not significantly affect the radio–to–X-ray flux correlation.

There is very little correlation between radio and X-ray source intensities shown in Fig. 6. Of the sources observed at both radio and X-ray frequencies, the strongest at both frequencies tend to be SNRs. Breaking the sample of 483 radio sources into those above the X-ray threshold of 0.002 counts s^{-1}(71 sources) and those below (412 sources), the fraction of SNRs is 51% (36 out of 71) and 6% (26 out of 412), respectively.

Similar results can be seen in Fig. 7 where we compared the 27 sources in common towards the SMC. Seventeen of the SMC sources (SNRs and H II regions) are stronger emitters in both radio and X-ray frequencies than eight background and two unclassified sources.

We followed the classification of Chu & Kennicutt (1988b) for SNRs in the LMC as Population I or Population II, to consider the difference in X-ray and radio properties of the two types. In Fig. 8 the X-ray Count Rate is plotted against the radio flux density (at 4.75 GHz) for

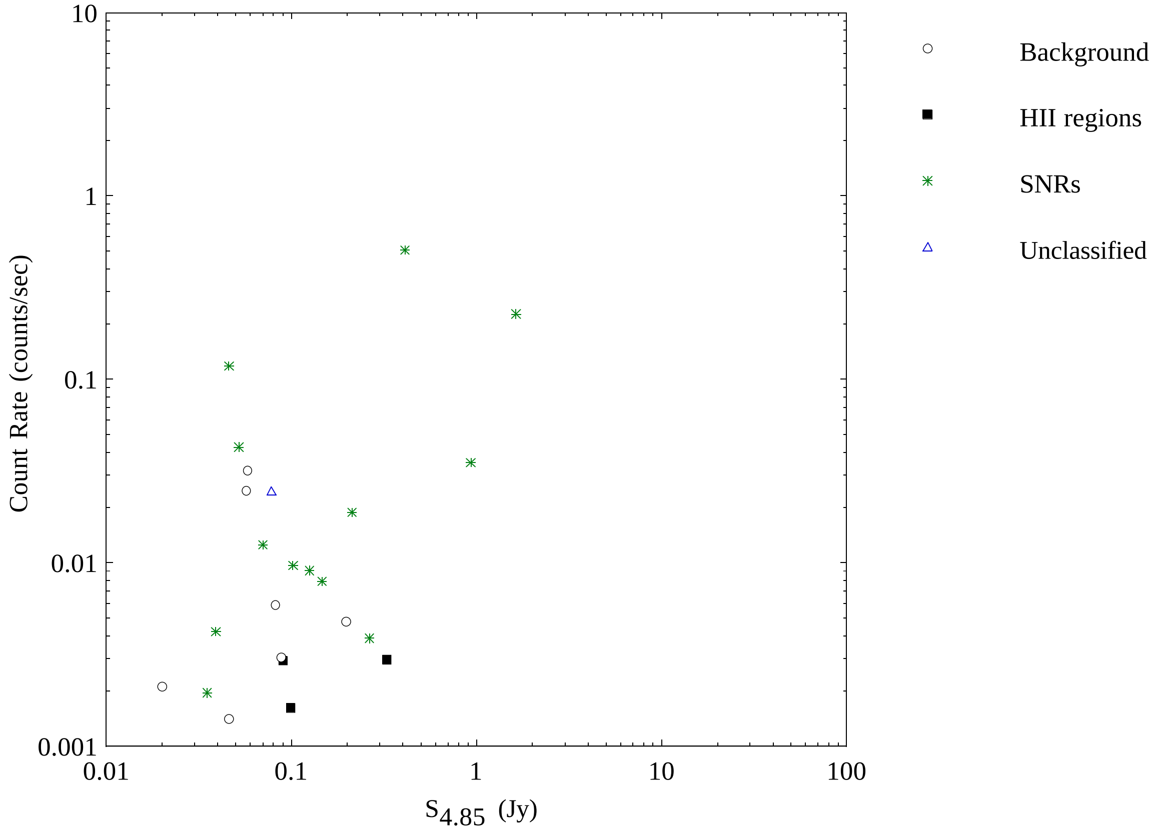

Fig. 7. The distribution of X-ray count rate and radio flux density at 4.85 GHz for different classes of sources in the SMC. Asterisks represent SNRs; filled squares – H II regions regions; open circles – background sources and open triangles – unclassified sources

32 SNRs distinguished by type. Nine SNRs are plotted as "unknown" types. The interpolated 4.75 GHz flux densities were estimated from other radio data for eight sources (flagged in Table 2, Col. 4) where no 4.75 GHz flux densities are available. There is a large scatter in the ratio of X-ray count rate to radio flux density. The ratio varies by three orders of magnitude from 0.019 to 18 counts s^{-1} Jy^{-1} with median 0.38 counts s^{-1} Jy^{-1} for the SNRs detected both at radio and X-ray. If we consider SNRs detected at radio but not in X-ray, the range of X-ray–to–radio ratio is even larger, with an upper limit as low as $5\ 10^{-4}$ counts s^{-1} Jy^{-1}. However, there is a tendency for SNRs which are strong in the radio to be also strong in X-rays.

Figure 8 shows that young SNRs from Population I appear in the top right-hand corner with strong X-ray and radio intensities. Dividing this sample at arbitrary values of 0.1 Jy and 0.1 counts s^{-1}, we note that the quadrant with strong radio and X-ray intensities is dominated by SNRs of Population I. Here 89% (8 out of 9) are Population I while in the other quadrants the fraction is 19% (6 out of 32) for the quadrant of strong radio and weak X-ray (including the sources below the X-ray threshold), 19% (3 out of 16) for weak radio, weak X-ray (including the sources below both thresholds) and 20% (1 out of 5) for weak radio, strong X-ray (including the sources below the radio threshold).

Population I SNRs are young and usually occur within large H II regions. This could be one reason for the occasional detection of X-ray emission from H II regions. Young Population II SNRs in the LMC are usually Balmer-dominated and occur in regions not interacting with other sources. They are, therefore, relatively weak X-ray and radio emitters. This could be a significant fact in SNR evolution; however, we can not rule out selection effects or a bias resulting from the small number of classified SNRs.

6. Conclusions

From a comparison of radio and X-ray surveys of the MCs we find 71 sources in common towards the LMC and 27 sources in common towards the SMC. The sources in common towards the LMC are mainly SNRs and SNR candidates (36) and background sources (27). Out of 27 sources in common in the field of the SMC, 14 are SNRs, three are H II regions and eight are background sources.

We used the X-ray hardness ratio 2 (HR2) to help classify radio sources as SNRs or background sources using the

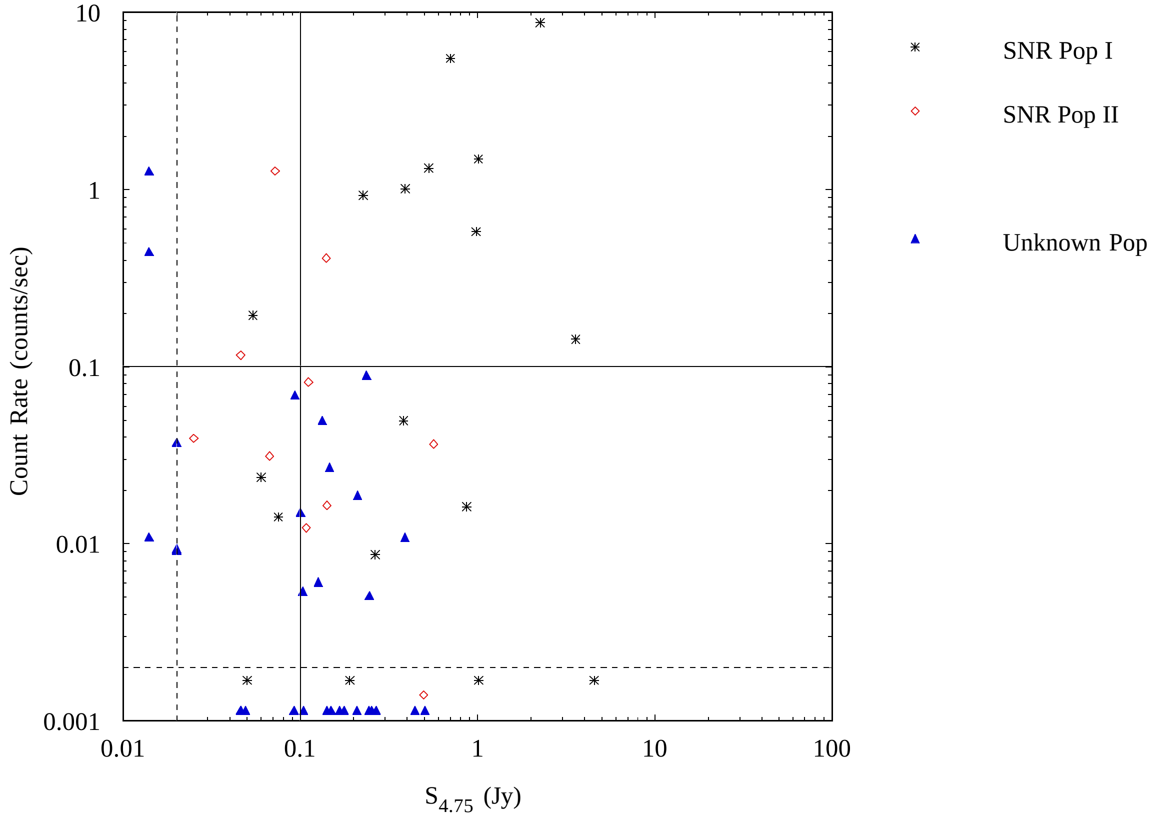

Fig. 8. The distribution of X-ray count rate and radio flux density at 4.75 GHz for different population of LMC SNRs. Asterisks represent Population I SNRs; open diamonds – Population II SNRs; and filled triangles SNRs of unknown population. Population I SNRs tend to be strong in both radio and X-ray surveys. The sample of sources with both strong radio and X-ray intensities is dominated by Population I SNRs

fact that the previously known background sources have positive HR2.

Based on this classification we propose six new radio and X-ray sources as SNR candidates in the LMC (LMC B0530−6655, LMC B0534−7204, LMC B0528−6838, LMC B0542−6702, LMC B0544−6910, LMC B0544−7030). Two SMC sources (SMC B0043−7330 and SMC B0054−7235) show characteristics typical for SNRs and therefore we classified them as SNR candidates.

From the number and radio flux densities of the LMC SNRs we derive an SNR birth-rate of one every 100(±20) yr and an SFR of 0.7 (±0.2) $M_\odot\,\mathrm{yr}^{-1}$ for the LMC. Similarly, for the SMC SNRs we find a birth-rate of one every 350 (±70) yr and an SFR of 0.15 (±0.05) $M_\odot\,\mathrm{yr}^{-1}$.

Comparing the intensities (radio and X-ray) for the sources in common towards the MCs, we found very little correlation between radio and X-ray intensities densities but note that the strongest SNRs from this sample are young SNRs from Population I.

Acknowledgements. M.D.F. acknowledges an Australian Government Overseas Postgraduate Research Scholarship and considerable support from the Australia Telescope National Facility (CSIRO), the Max-Planck-Institut für Extraterrestrische Physik (MPE) and Max-Planck-Institut für Radioastronomie (MPIfR). This work is also supported by the Australian Research Council (ARC) and the ROSAT project is supported by the German Bundesministerium für Bildung, Wissenschaft, Forschung und Technologie (BMBF/DARA) and the Max-Planck-Gesellschaft. We thank J. Lequeux, Y.H. Chu, M. Ehle, D. Goddard, L. Staveley-Smith, D. Hartmann and J. Trümper for considerable support and comments on the manuscript.

References

Amy S.W., 1994, Proc. ASA 11(1), 83
Arthur S.J., Henney W.J., 1996, ApJ 457, 752
Aschenbach B., 1995, in: Makino F., Ohashi T. (eds.) New horizon of X-ray Astronomy, Proceedings of the International Conference on X-ray Astronomy. Universal Academy Press, Tokyo, Japan, p. 103
Bolton J.G., Butler P.W., 1975, Aust. J. Phys. Suppl. 34, 33
Bruhweiler F.C., Klinglesmith D.A., Gull T.R., Sofia S., 1987, ApJ 317, 152
Caplan J., Deharveng L., 1985, A&AS 62, 63
Caplan J., Deharveng L., 1986, A&A 155, 297
Caplan J., Ye T., Deharveng L., Turtle A.J., Kennicutt R.C., 1996, A&A 307, 403
Chu Y.H., Kennicutt R.C., 1988a, AJ 95(4), 1111

Chu Y.H., Kennicutt R.C., 1988b, AJ 96, 1874
Chu Y.H., Wakker B., Low M.M.M., 1990, ApJ 365, 510
Chu Y.H., Low M.M.M., Garcia-Segura G., Wakker B., Kennicutt R.C., 1993, ApJ 414, 213
Chu Y.H., Kennicutt R.C., 1994, ApJ 425, 720
Chu Y.H., Wakker B., Low M.M.M., Garcia-Segura G., 1994, AJ 108, 1696
Chu Y.H., Dickel J.R., Staveley-Smith L., Osterberg J., Smith C.R., 1995a, AJ 109, 1729
Chu Y.H., Chang H.W., Su Y.L., Low M.M.M., 1995b, ApJ 450, 157
Chu Y.H., Kennicutt R.C., Snowden S.L., et al., 1997, PASP (in press)
Clarke J.N., 1976, MNRAS 174, 393
Clarke J.N., Little A.G., Mills B.Y., 1976, Aust. J. Phys. Suppl. 40, 1
Cohen R., Dame T.M., Garay G., et al., 1988, ApJ 331, L95
Condon J.J., 1992, ARA&A 30, 575
Corwin H.G., de Vaucouleurs A., de Vaucouleurs G., 1985, Southern Galaxy Catalogue, Austin
Davies R.D., Elliott K.H., Meaburn J., 1976, Mem. R. Astr. Soc. 81, 89
DeGioia-Eastwood K., 1992, ApJ 397, 542
Dennefeld M., 1982, A&A 157, 267
Dickel J.R., Milne D.K., Junkes N., Klein U., 1993, A&A 275, 265
Dickel J.R., Milne D.K., 1994, Proc. ASA 11, 99
Dickel J.R., Milne D.K., Kennicutt R.C., Chu Y.H., Schommer A., 1994, AJ 107(3), 1067
Dickel J.R., Milne D.K., 1995, AJ 109, 200
Dickel J.R., Chu Y.H., Gelino C., et al., 1995, ApJ 448, 623
Dickey J.M., Amy S., Haynes R.F., et al., 1994, A&A 289, 357
Dopita M.A., Tuohy I.R., Mathewson D.S., 1981, ApJ 248, L105
Filipović M.D., 1996, PhD Thesis, University of Western Sydney, Nepean
Filipović M.D., Haynes R.F., White G.L., et al., 1995, A&AS 111, 311 (Paper IV)
Filipović M.D., White G.L., Haynes R.F., et al., 1996, A&AS 120, 77 (Paper IVa)
Filipović M.D., White G.L., Haynes R.F., et al., 1997a, A&AS 121, 321 (Paper V)
Filipović M.D., Haynes R.F., White G.L., Jones P.A., 1997b, A&A (submited) (Paper VII)
Graham J.R., Evans A., Albinson J.S., Bode M.F., Meikle W.P.S., 1987, ApJ 319, 126
Haynes R.F., Klein U., Wayte S.R., et al., 1991, A&A 252, 475
Helfand D.J., 1991, in: Haynes R.F., Milne D.K. (eds.) Proc. IAU Symp. 148, The Magellanic Clouds. Reidel, Dordrecht, p. 37
Henize K.G., 1956, ApJS 2, 315
Hodge P.W., Snow T.P., 1975, AJ 80, 9
Hughes P. J., et al., 1995, ApJ 444, L81
Hunt M.R., Whiteoak J.B., 1994, Proc. ASA 11, 68
Hwang U., Hughes J.P., Canizares C.R., Markert T.H., 1993, ApJ 414, 219
Inoue H., Koyama K., Tanaka Y., 1983, in: Danziger I.J., Gorenstein P. (eds.) Proc. IAU Symp. 101, Supernova Remnants and their X-Ray Emission. Reidel, Dordrecht, p. 535
Israel F.P., Johansson L.E.B., Lequeux J., et al., 1993, A&A 276, 25
Israel F.P., Maloney P.R., Geis N., et al., 1996, ApJ 465, 738
Jones T.J., Hyland A.R., Straw S., et al., 1986, MNRAS 219, 603
Jones P.A., McAdam W.B., 1992, ApJS 80, 137
Kahabka P., et al. (in preparation)
Kennicutt R.C., 1991, in: Haynes R.F., Milne D.K. (eds.) Proc. IAU Symp. 148, The Magellanic Clouds. Reidel, Dordrecht, p. 139
Laustsen S., Madsen C., West R.M., 1987, Exploring the Southern Sky. Springer Verlag, Berlin
Laval A., Rosado M., Boulesteix J., et al., 1989, A&A 208, 230
Laval A., Rosado M., Boulesteix J., et al., 1992, A&A 253, 213
Long K.S., Helfand D.J., Grabelsky D.A., 1981, ApJ 248, 925
Lucke P.B., Hodge P.W., 1970, AJ 75(2), 171
Manchester R.N., Staveley-Smith L., Kesteven M.J., 1993, ApJ 411, 756
Massey P., Lang C.C., DeGioia-Eastwood K., Garmany C.D., 1995, ApJ 438, 188
Mathewson D.S., Ford V.L., Dopita M.A., et al., 1983, ApJS 51, 345
Mathewson D.S., Ford V.L., Dopita M.A., et al., 1983a, in: Danziger J., Gorenstein P. (eds.) Proc. IAU Symp. 101, Supernova Remnants and their X-Ray Emission. Reidel, Dordrecht, p. 541
Mathewson D.S., Ford V.L., Dopita M.A., et al., 1984, ApJS 55, 189
Mathewson D.S., Ford V.L., Tuohy I.R., et al., 1985, ApJS 58, 197
McGee R.X., Milton J.A., 1966, Aust. J. Phys. Suppl. 51, 345
McGee R.X., Brooks J.W., Batchelor R.A., 1972a, Aust. J. Phys. 25, 581
McGee R.X., Brooks J.W., Batchelor R.A., 1972b, Aust. J. Phys. 25, 613
McGee R.X., Newton M.L., 1972, Aust. J. Phys. 25, 619
McGee R.X., Newton L.M., Butler P.W., 1976, Aust. J. Phys. 29, 329
Meaburn J., Laspias V.N., 1991, A&A 245, 635
Mills B.Y., Little A.G., Durdin J.M., Kesteven M.J., 1982, MNRAS 200, 1007
Mills B.Y, Turtle A.J., Little A.G., Durdin M.J., 1984, Aust. J. Phys. 37, 321
Milne D.K., Caswell J.L., Haynes R.F., 1980, MNRAS 191, 469
Mountfort P.I., Jonas J.L., de Jager G., Baart E.E., 1987, MNRAS 226, 917
Otrupcek R.E., Wright A.E., 1991, Proc. ASA 9, 170
Pietsch W., et al. (in preparation)
Pietsch W., Kahabka P., 1993, in: Baschek B., Klare G., Lequeux J. (eds.) Proc. of the Second European Meeting on the Magellanic Cloud 328, New Aspects of Magellanic Cloud Research. Reidel, Dordrecht, p. 59
Pizzichini G., Cline T.L., Desai U.D., et al., 1983, in: Danziger J., Gorenstein P. (eds.) Proc. IAU Symp. 101, Supernova Remnants and their X-Ray Emission. Reidel, Dordrecht, p. 573
Rosa M.R., 1993, in: Baschek B., Klare G., Lequeux J. (eds.) Proc. of the Second European Meeting on the Magellanic Cloud 328, New Aspect of Magellanic Cloud Research. Reidel, Dordrecht, p. 145
Rosado M., Laval A., le Coarer E., et al., 1993a, A&A 272, 541

Rosado M., Le Coarer E., Georgelin Y.P., Viale A., 1993b, in: Bachek B., Klare G., Lequeux J. (eds.) Proc. of the Second Europian Meeting on the Magellanic Cloud 328, New Aspect of Magellanic Cloud Research. Reidel, Dordrecht, p. 36
Rosado M., Le Coarer E., Georgelin Y.P., 1994, A&A 286, 231
Sanduleak N., 1984, in: Van den Bergh S., de Boer K.S. (eds.) Proc. IAU Symp. 108, Structure and Evolution of the Magellanic Clouds. Reidel, Dordrecht, p. 231
Sanduleak N., MacConnell D.J., Davis Philip A.G., 1978, PASP 90, 621
Savage A., 1976, MNRAS 174, 259
Savage A., Bolton J.G., Wright A.E., 1977, MNRAS 179, 135
Schwering P.B.W., Israel P.F., 1991, A&A 246, 231
Seward F.D., Mitchell M., 1981, ApJ 243, 736
Shull P. Jr., 1983, ApJ 275, 592
Sinnott R.W., 1988, NGC 2000. Cambridge University Press, p. 46
Smith R.C., Chu Y.H., Low M.M.M., Oey M.S., Klein U., 1994, AJ 108, 1266
Snowden S. L., Petre R., 1994, ApJ 436, L123
Staveley-Smith L., Sault R.J., Hatzidimitriou D., Kesteven M.J., McConell D., et al., 1997, MNRAS (in press)
Taylor J.H., Manchester R.N., Lyne A.G., 1993, ApJS 88, 529
Trümper J., Hasinger G., Aschenbach B., et al., 1991, Nat 349, 579
Tuohy I.R., Dopita M.A., Mathewson D.S., Long K.S., Helfand D.J, 1982, ApJ 261,473
Tuohy I.R., Dopita M.A., Mathewson D.S., Long K.S., Helfand D.J, 1983, in: Danziger J., Gorenstein P. (eds.) Proc. IAU Symp. 101, Supernova Remnants and their X-ray Emission. Reidel, Dordrecht, p. 559
Van Buren D., Greenhouse M.A., 1994, ApJ 431, 640
Vancura O., Blair W.P., Long K.S., Raymond J.C., 1992, ApJ 394, 158
Wang Q., Hamilton T., Helfand D.J., Wu X., 1991, ApJ 374, 475
Wang Q., Helfand D.J., 1991a, ApJ 370, 541
Wang Q., Helfand D.J., 1991b, ApJ 373, 497
Wang Q., Wu X., 1992, ApJS 78, 391
Westerlund B.E., 1993, in: Baschek B., Klare G., Lequeux J. (eds.) Proc. of the Second European Meeting on the Magellanic Cloud 328, New Aspects of Magellanic Cloud Research. Reidel, Dordrecht, p. 7
White G.L., Batty M.J., Bunton D.J., Brown D.R., Corben J.B., 1987, MNRAS 227, 705
White G.L., Bunton D.J., Anderson M.W.B., et al., 1991, MNRAS 248, 398
Whithfield G.R., 1957, MNRAS 117, 680
Wilcots E.M., 1994, AJ 107(4), 1338
Williams R.M., et al., 1997, ApJ (in press)
Wright A.E., Griffith M., Burke B., Ekers R.D., 1994, ApJS 91, 111
Ye T., 1988, PhD Thesis, Sydney University
Ye T., Turtle A.J., Kennicutt R.C., 1991, MNRAS 249, 722
Ye T., Amy S.W., Wang Q.D., Ball L., Dickel J., 1995, MNRAS 275, 1218